Class.Q.Grav. Vol.15(1998) pp.3085–3120. 26-Dec-1996

Riemann Normal Coordinates, Smooth Lattices and Numerical Relativity

Leo Brewin

Department of Mathematics
Monash University
Clayton, Vic. 3168
Australia

Abstract

A new lattice based scheme for numerical relativity will be presented. The scheme uses the same data as would be used in the Regge calculus (eg. a set of leg lengths on a simplicial lattice) but it differs significantly in the way that the field equations are computed. In the new method the standard Einstein field equations are applied directly to the lattice. This is done by using locally defined Riemann normal coordinates to interpolate a smooth metric over local groups of cells of the lattice. Results for the time symmetric initial data for the Schwarzschild spacetime will be presented. It will be shown that the scheme yields second order accurate estimates (in the lattice spacing) for the metric and the curvature. It will also be shown that the Bianchi identities play an essential role in the construction of the Schwarzschild initial data.

PACS numbers: 04.25.Dm, 04.60.Nc, 02.70.-c

1. Introduction

One of the most common techniques employed in numerical general relativity is that of finite differences. In this approach the coordinate components of the metric are sampled at a series of well defined points. The connection and curvatures are then calculated from well known finite difference formulae. Such formula can be easily derived in a number ways, and in particular, by way of a quadratic interpolation of the sampled values. Though this method has produced excellent results it is reasonable to explore other alternatives.

The alternative to be developed in this paper is to use a lattice of geodesic segments to provide the samples of the spacetime metric. The curvature will, as with finite differences, be obtained from a quadratic interpolation of the sampled metric. This procedure is, however, somewhat more involved than that for finite differences.

Lattice theories of general relativity such as the Regge calculus [1] are not particularly new. What makes our approach new is the way in which the discrete fields equations are constructed from the lattice variables such as the leg lengths. In the Regge calculus this is done by way of an action integral whereas in our approach the field equations of general

relativity are applied directly to the lattice. We will defer further comparison of the Regge calculus with our approach until after the main results of this paper have been presented.

For any explicitly given spacetime it is straightforward, though perhaps computationally tedious, to construct a lattice of geodesic segments (eg. by sub-dividing the spacetime into a set of simplices). This lattice will inherit information about the topology and geometry of the parent spacetime. If the lattice is chosen correctly then it is possible to record all of the topological information of the parent spacetime in the lattice. The same is not true for the metric since the lattice contains only a finite number of geodesic segments. Thus some information will be lost in going from the parent spacetime to the lattice. The interesting question is how much information about the parent spacetime can be recovered from the lattice? In particular, can the lattice be used to estimate the curvature tensor of the spacetime, and if so, with what accuracy? One can expect that the answer to this question will entail, just as in the finite difference case, a locally quadratic interpolation of the sampled data.

For the moment suppose that such an interpolation procedure exists (while putting aside the issue of accuracy). Then given a set of leg lengths one can compute an associated set of curvatures. Einstein's equations can then be evaluated and the leg lengths adjusted accordingly. Clearly this amounts to solving Einstein's equations for the parent spacetime discretised on a lattice. This is the basis for using lattices – they provide an alternative to finite differences as a tool for numerical relativity.

The procedure for estimating the curvatures from the leg lengths will be based on Riemann normal coordinates [2-5] (later referred to as RNC). A simple algebraic definition of these coordinates is that, for a given point O, they are a local set of coordinates, such that

$$\Gamma^{\mu}_{\alpha\beta} = 0$$

$$\Gamma^{\mu}_{\alpha\beta,\nu} + \Gamma^{\mu}_{\beta\nu,\alpha} + \Gamma^{\mu}_{\nu\alpha,\beta} = 0$$

at O.

An equivalent and perhaps more instructive geometric definition goes as follows. Consider the point O and a small neighbourhood of O. If P is any other point near to O then there exists a unique geodesic joining O to P. Let a^{μ} be the components of the unit vector to this geodesic at O and let s be the geodesic length from O to P. Then the Riemann normal coordinates of P are defined to be $x^{\mu} = sa^{\mu}$. This construction fails whenever the geodesic joining O to P is not unique (ie. when geodesics cross). Fortunately the neighbourhood of O can always be chosen to be small enough so that this problem does not arise. Incidentally, this displays the local nature of Riemann normal coordinates. They cannot be used to cover the whole manifold. Instead a collection of distinct Riemann normal coordinates must be constructed.

From this simple definition a number of very useful theorems can be proved (see the Appendix). In particular, for the parent spacetime, the metric is of the form

$$g_{\mu\nu}(x) = g_{\mu\nu} - \frac{1}{3} R_{\mu\alpha\nu\beta}\, x^\alpha x^\beta + \mathcal{O}(\epsilon^3) \tag{1.1}$$

where $g_{\mu\nu}$ and $R_{\mu\alpha\nu\beta}$ are the components of the metric and Riemann tensors at the origin O of the RNC and and ϵ is a typical length scale of the neighbourhood in which the RNC is defined. This equation is nothing more than a Taylor series expansion of the metric around the origin O. Higher order approximations can be generated by continuing the series. The question of convergence is not very important in our context because we can always choose the domain of the RNC sufficiently small so that the truncation error in the above expansion is negligible. Note that the above expansion can be viewed as a flat space part (the constant term) plus a small perturbation (the curvature term).

From this metric one can derive formulae for such things as the length of a geodesic segment and the angle subtended at the vertex of a geodesic triangle. The length of a geodesic segment with vertices i and j is given by

$$L_{ij}^2 = g_{\mu\nu} \Delta x_{ij}^\mu \Delta x_{ij}^\nu - \frac{1}{3} R_{\mu\alpha\nu\beta}\, x_i^\mu x_i^\nu x_j^\alpha x_j^\beta + \mathcal{O}(\epsilon^5) \tag{1.2}$$

while the angle, θ_k, subtended at the vertex k of the triangle with vertices i, j and k can be computed from

$$2 L_{ik} L_{jk} \cos\theta_k = L_{ik}^2 + L_{jk}^2 - L_{ij}^2 - \frac{1}{3} R_{\mu\alpha\nu\beta}\, \Delta x_{ik}^\mu \Delta x_{ik}^\nu \Delta x_{jk}^\alpha \Delta x_{jk}^\beta + \mathcal{O}(\epsilon^5) \tag{1.3}$$

These formulae can be easily applied if we are given the various $g_{\mu\nu}, R_{\mu\nu\alpha\beta}$ and x_i^μ of the parent spacetime. However, we wish to pose the inverse problem, given just the leg lengths, angles and the combinatoric information of a lattice, compute (or estimate) the curvature of the parent spacetime. This can be done by treating the above as a coupled system of non-linear equations. There is one such system of equations for each vertex.

We will define a *smooth lattice* to be a lattice for which we have solved the above equations, (1.2) and (1.3), which in turn will be referred to as the *smooth lattice equations*. (Though a better choice might be *Riemann lattice*.)

There are a number of attractive features in the smooth lattice approach that deserve special mention. First, we have made explicit use of the equivalence principle by setting the connection to zero at the origin of each RNC. This not only simplifies many calculations but it also allows us to interpret each RNC as a locally freely falling frame. This central use of the equivalence principle must surely be to our advantage. The second point is that the smooth lattice equations are very easy to formulate and solve. In contrast, the equations in the Regge calculus are very tedious with numerous inverse trigonometric and hyperbolic functions and are far from simple to setup and evaluate on a computer. Solving the Regge

equations on a computer could easily be a very time consuming task (much more so than either for finite differences or for our method). The third point is that as our method has a solid theoretical basis we are able to use all of the usual tools of differential geometry and analysis to investigate issues such as convergence and discretisation errors. Such is not the case with the Regge calculus.

Despite these attractive features one cannot apply the method naively. In any practical application one may need to address the following issues (amongst others).

- ◇ *Over which region should each RNC be defined?* To each vertex there should be assigned a set of simplices from which the information is to be extracted. The size of that region (ie. the number of simplices) must reflect the amount of information required. It seems that the smallest practical region would be that composed of the ball of simplices attached to the nominated vertex.

- ◇ *Are there any gauge freedoms in choosing the RNC?* Yes, for example the standard rotations, translations etc. This gauge freedom can be used to force $g_{\mu\nu}$ and or various x_i^μ to take on specific values. The remaining quantities must be computed together with the curvatures from the smooth lattice equations.

- ◇ *Are there as many equations as unknowns?* Yes, but only in two dimensions and only when the surface consists of triangles. In higher dimensions the set of equations is usually overdetermined. This problem can be overcome by either resorting to a least squares solution or by simply excluding some of the equations. Another option would be to increase the number of parameters, such as derivatives of the curvature, in the interpolation of the metric so as to produce a properly determined set of equations.

- ◇ *Is there a unique solution to the smooth lattice equations?* In general, no – the smooth lattice equations are non-linear and so we can expect more than one solution. The members of a discrete family of solutions will most probably be related by discrete transformations such as folding one simplex over another. We would hope that there would be one exceptional case where all the simplices do not overlap and this would be the solution we would choose. There is also the possibility of having a continuous family of solutions. This would suggest that the lattice is improperly defined in that it lacks sufficient structure (eg. too few leg lengths). This later case should not be allowed to occur in practice.

- ◇ *Can all of the leg lengths and angles be freely chosen?* If the curvatures are specified locally, as they are in our system of RNC's, then there is question as to whether or not there exists a single metric which has a curvature matching the specified local values. This is nothing more than a question of integrability – given a curvature tensor does there exist a corresponding metric? The answer is yes provided that that curvature satisfies the Bianchi identities. For our set of RNC's this imposes (surprisingly) a set of constraints on the choice of the leg lengths and angles.

Some of these issues will be explored in greater detail in later sections.

2. Schwarzschild initial data

As a test of the smooth lattice method we should be able to successfully recover the time symmetric 3-geometry for the Schwarzschild spacetime. This metric can be written in the form

$$ds^2 = dl^2 + \eta(l)^2\, d\Omega^2$$

where l is the proper distance measured from the throat, $\eta(l)$ is a smooth function of l and $d\Omega^2$ is the standard metric of a unit 2-sphere.

We will present two examples of a smooth lattice discretisations of this metric. In the first example we will discretise the metric of the unit 2-sphere while retaining a continuous radial coordinate. We will first use the smooth lattice method to estimate the curvature of a unit 2-sphere (for which we all know the exact value, 2). This estimate will then be used in a radial integration of the Hamiltonian constraint to complete the construction of the 3-metric.

This is a very simple test of the method. A much stronger test will be presented in our second example where the full 3-metric will be discretised (though we will use the spherical symmetry to simplify the calculations).

2.1. Smooth lattice 2-sphere

The smooth lattice equations will be used in this example solely as a means to estimate the Riemann curvature scalar of a unit 2-sphere. This is known to have the value 2 so this may appear to be a somewhat unnecessary application of the method. However, if the method fails in this simplest of all cases then it surely will be of little use in any other situation. Once the curvature has been estimated we will employ it in solving the standard time symmetric constraint equations for the three metric.

We will estimate R from the known 2-metric of the unit 2-sphere. To do so it will be necessary to choose a lattice on the 2-sphere, compute the geodesic leg lengths and finally solve a set of equations (given below) for R.

The simplest approximation to a 2-sphere is a regular tetrahedron (see Figure (1)). This cannot be expected to provide very accurate estimates for the curvature. Thus some scheme for refining the lattice will be required. The scheme used in this example will be to successively sub-divide each triangle according to the pattern in Figure (2).

The metric of the 2-sphere can be written as

$$ds^2 = d\theta^2 + \sin^2\theta\, d\phi^2$$

or as the induced metric on the surface $1 = x^2 + y^2 + z^2$ in Euclidean 3-space with the usual (x, y, z) coordinates. The (θ, ϕ) and (x, y, z) coordinates are related by the usual polar coordinate transformations. The (x, y, z) coordinates of the four vertices of the original tetrahedron are easily calculated by appealing to the symmetry of the (regular) tetrahedron.

The coordinates of the vertices of the successive lattices are calculated in a two step process. First each new vertex is introduced to the centre of each old leg. This vertex is then displaced along the radial direction out to the unit sphere. In this way the (θ, ϕ) coordinates of each vertex can be calculated.

The leg lengths for each leg are calculated by solving the geodesic equations on the 2-sphere as a two point boundary value problem. At the same time we compute $\int ds$ along this geodesic path. This gives us the leg lengths for each geodesic segment. We then discard the continuum metric and turn to the smooth lattice equations to estimate R.

2.2. Smooth lattice equations

Consider the Riemann normal coordinate frame centred on vertex O. Suppose there are n triangles attached to this vertex and that the vertices, starting with O, are labelled, 0 to n.

We are free to choose our Riemann normal coordinates such that $g_{\mu\nu}(x_o) = \mathrm{diag}(1, 1)$, $(x_o^\mu) = (0, 0)$ and $(x_1^\mu) = (\star, 0)$ where $\star$ denotes a number to be computed from the smooth lattice equations. This exhausts all coordinate freedoms, and thus all of the remaining x_i^μ and curvature components must be computed from the given leg lengths and the smooth lattice equations (1.2). These equations were applied only to the legs of the triangles attached to O. Note that in 2-dimensions, there is only one independent curvature component, which we can take to be R_{1212}.

Since there are n triangles attached to O, there will be $2n$ leg lengths L_{ij}. There are also $n+1$ vertices for which there are $2(n + 1)$ coordinates x_i^μ to compute. However, we have already chosen 3 of the $2(n + 1)$ coordinates. Thus we have to compute $2n - 1$ coordinates and one curvature component from the $2n$ leg lengths L_{ij}. Fortunately, we have as many equations as unknowns. (In fact it is easy to see that this will always be true in 2-dimensions, provided the surface is fully triangulated.) For each of our sub-divisions we have four vertices with $n = 3$ and the remainder with $n = 6$.

The $2n$ equations (1.2) were solved for the x_i^μ and R_{1212} via a Newton-Raphson method. Starting from flat space, the iterations converged in about 3-4 iterations (though more iterations were required for the very coarse approximations of the original tetrahedron).

The estimates so obtained are listed in Table (1). Since not every vertex in each approximation is equivalent to every other vertex (they have differing local triangulations) the method returns different estimates for R for each vertex. Hence in the table we have listed the best and worst estimates for R. One can observe that the method converges by a factor of four with each successive sub-division. As the leg lengths are halved with each sub-division this implies the error in R varies as $\mathcal{O}(L^2)$ where L is a typical length scale for leg lengths. That is, the smooth lattice yields 2nd-order accurate estimates for the curvature.

Table 1. Estimates of $\lvert R-2\rvert$ for a unit 2-sphere			
Sub-division	Worst estimate	Best estimate	Average estimate
1	1.19	1.19	1.19
2	2.99e-1	4.91e-2	1.71e-1
3	6.40e-2	1.91e-3	2.55e-2
4	1.54e-2	5.67e-5	2.97e-3
5	3.81e-3	5.18e-6	2.47e-4

2.3. The Hamiltonian constraint

Using the above values for R we can now proceed to the construction of the Schwarzschild 3-metric. Our starting point is to propose a 3-metric in the form

$$ds^2 = dl^2 + \eta(l)^2 \left(d\theta^2 + \sin^2\theta\, d\phi^2\right)$$

Where l is the radial proper distance measured from the throat. There is only one non-trivial constraint equation, the Hamiltonian constraint,

$$0 = {}^{(3)}R$$

which must be solved for $\eta(l)$. To begin, write the metric in the 2+1 form

$$(g_{\mu\nu}) = \begin{pmatrix} 1 & 0 \\ 0 & \eta^2 h_{\mu\nu} \end{pmatrix}$$

where $h_{\mu\nu}$ is the metric of the unit 2-sphere. Then it is a straightforward calculation to show that the Hamiltonian constraint is

$$\frac{d}{dl}\left(\frac{1}{\eta}\frac{d\eta}{dl}\right) = \frac{R}{4\eta^2} - \frac{3}{2}\left(\frac{1}{\eta}\frac{d\eta}{dl}\right)^2 \tag{2.3.1}$$

where R is the scalar curvature of the unit 2-sphere.

The boundary conditions at the throat, where $l = 0$, are chosen to be

$$\eta = 2 \qquad \text{and} \qquad \frac{d\eta}{dl} = 0 \tag{2.3.2}$$

The first condition is equivalent to setting the ADM mass to $m = 1$ (ie. $\eta = 2m$). The second condition is required for $l = 0$ to be a minimal surface.

Note that in the above equation R can take on any value not just the discrete values found in the previous section. As we have already seen that the smooth lattice method gives accurate and convergent estimates for R, we will in the following discussions allow R to take on any value in the range $2 \leq R \leq 3$.

For each choice of R the initial value problem (2.3.1) was solved using a 4-th order Runge Kutta method starting from the throat and integrating outwards. A step length of $dl = 0.2$ was used in each of the following calculations.

The result of the integration is that we have the 3-metric in the form

$$ds^2 = dl^2 + \eta^2(l)\, d\Omega^2 \tag{2.3.3}$$

where $d\Omega^2$ is the metric of the unit 2-sphere. We would like to compare this with the exact metric corresponding to $R = 2$. One easy way to do this is to integrate (2.3.1) again but this time with $R = 2$. This will yield a metric of the form

$$d\tilde{s}^2 = dl^2 + \tilde{\eta}^2(l)\, d\Omega^2 \tag{2.3.4}$$

The error can then be easily computed as

$$e(l, R) = -1 + \frac{\eta(l)}{\tilde{\eta}(l)} \tag{2.3.5}$$

The results are shown in Figures (3) and (4). The first graph shows that for a fixed value of R the error rises steeply from the throat and then settles to a constant value independent of l. This is easy to understand, it shows that in the distant almost flat regions of the metric the error in approximating a smooth 2-sphere with a smooth lattice does not depend on the size of the 2-sphere. This graph also shows that for any fixed l the error vanishes as $R \to 2$ (as it must). The second plot, Figure (4), is just a series of cross-sections of the first plot, Figure (3), at specific values of l. This graph clearly shows that the error in η, at a fixed l, appears to vary linearly with the error in R. Since we have previously established that the error in R varies as $\mathcal{O}(L^2)$ we can infer that the global discretization error in η appears to be $\mathcal{O}(L^2)$.

It should be noted that the metrics generated for various values of R are not isometric to each other. To see this note that (2.3.1) is symmetric under the transformation $R \to k^2 R$, $\eta \to k\eta$ for any k. Thus we can always scale R to $R = 2$. However the resulting re-scaling of η is, through the boundary condition (2.3.2), equivalent to changing the ADM mass. This proves the assertion. The upshot of this that there is no single method to compare two metrics with differing values of R. The method described above is just one of many possible ways to compare our approximate metric against the exact metric. If one is not careful it is possible to generate an apparently acceptable definition of the error which displays, for fixed R, an

error that diverges as $l \to \infty$. As an example, suppose we wrote our exact metric in the form

$$d\tilde{s}^2 = \rho^4(r)\left(dr^2 + r^2\, d\Omega^2\right)$$

where $\rho(r) = 1 + (m/2r)$. To compare this metric with our approximate metric (2.3.3) we could generate a transformation between the r and l coordinates by integrating, in parallel with the main equation (2.3.1),

$$\frac{dr}{dl} = \frac{r}{\eta} \tag{2.3.6}$$

starting from $r = m/2$ at $l = 0$. The error could then be defined as

$$e(l, R) = -1 + \frac{\eta(l)}{r(l)\rho(r(l))^2} \tag{2.3.7}$$

The results are displayed in Figure (5) and clearly display the stated divergence. However, at a fixed value of l we find, see Figure (6), that the error vanishes as $R \to 2$, ie. at each physical point the approximate metric converges to the exact metric.

Note that in this example all that we have changed is the way in which the two metrics are compared. Why did the first method work so much better than the second? The answer lies in the choice of the transformation (2.3.6). This contains the function η which is only an approximation to the exact $\tilde{\eta}$. The result is that r and l are not properly aligned. What this means is the following. To each metric we can compute the proper distance from the throat to any point in question. For ds the distance to the point with coordinate l is just l. For the exact metric $d\tilde{s}$ the distance is $\tilde{l}(r) = \int_{m/2}^{r} \rho^2(u)\, du$ for the point with coordinate r. The above transformation (2.3.6) does not produce $l = \tilde{l}(r)$. In fact, when both l and $\tilde{l}$ are large,

$$\frac{d\eta}{dl} \sim \sqrt{\frac{R}{2}}\,, \qquad\qquad \frac{d\tilde{\eta}}{d\tilde{l}} \sim 1$$

which when combined with the above (2.3.6) and $dr/d\tilde{l} = r/\tilde{\eta}$ leads to

$$\tilde{l} \sim l^{\sqrt{2/R}}$$

Thus $\tilde{l} - l$ diverges (for $R \neq 2$) as $l \to \infty$. This is the source of the apparent divergence in the metrics (for fixed R). In contrast, the original definition of the error (2.3.5) does not suffer from this problem because it compares the metric coefficients η and $\tilde{\eta}$ at the same proper distance from their respective throats.

An honest assessment of the above example is that even though it has given the correct answers it must be viewed as a very benign test of the smooth lattice method. The sole contribution of the smooth lattice was to aid in the computation of the scalar 2-curvature, which was already known to be 2. One could probably concoct any number of schemes which

spit out the magic number 2. A far better test would be to use the smooth lattice approach to fully discretise the 3-metric. This brings us to our second example.

3. Fully discretised 3-metric

Our aim in this example is to subject the smooth lattice approach to a much more stringent test than that used in the previous example. We will base our test on a fully discretised three dimensional lattice. Our plan of attack is as follows. First, we will choose the structure of our lattice. Coordinate and gauge conditions that reflect the desired spherical symmetries will then be imposed after which the smooth lattice equations will be written out in full. Finally we will argue that the Bianchi identities will need to be imposed so as to produce a set of equations from which the correct metric can be obtained.

Consider now the construction of a lattice for a spherically symmetric space. An extreme example would be to choose a lattice in which the vertices have been randomly scattered throughout the space. This is not only impractical but it also fails to take advantage of the obvious symmetries of the space. We will instead choose a lattice (see Figures (7,8)) built from a single tube stretching from the throat out to the distant flat regions of the space. The tube has a rectangular cross-section and it is subdivided into a sequence of cube like cells. Each cell stretches from one 2-sphere to the next and each successive pair of cells defines the domain of each RNC. The four edges of the tube, not just the radial edges of the cells, will be required to be global radial geodesics. It is important to note that the rectangular tiles such as that defined by the vertices 1,2,3 and 4, do not lie in the 2-spheres (except at the throat). The edges such as $(1, 2)$ are geodesic segments of the full 3-metric and thus cannot also be geodesic segments of the 2-spheres.

Though we have only constructed one tube we will assume, on the basis of spherical symmetry, that it captures all of the important geometric information of the 3-metric. Thus there is no need to replicate this tube through out the space.

Let us now turn to the issue of coordinate and gauge conditions. This will entail arranging our RNC in each pair of cells, imposing restrictions on the curvature components and imposing the gauge condition that the radial edges of the tube are global geodesics.

We are free to choose an orthonormal RNC frame at the origin. Thus $g_{\mu\nu} = \mathrm{diag}(1, 1, 1)$ at the origin. The Riemann normal coordinates for the vertices in each pair of cells were chosen as per Table (2). This choice can be achieved as follows. First align the z-axis with the radial geodesic running up the centre of the tube. The origin can then be slid up and down this geodesic to set the z coordinates of vertices 1,2,3 and 4 to zero. Finally, by a suitable rotation about the z-axis, the remaining pattern amongst the x and y coordinates can be achieved.

Table 2. Coordinates for the vertices in Figure (8)

Vertex	(x^μ)	**Vertex**	(x^μ)	**Vertex**	(x^μ)
1^-	$(\ a^-,\ \ a^-,\ b^-)$	1	$(\ a,\ \ a,\ 0)$	1^+	$(\ a^+,\ \ a^+,\ b^+)$
2^-	$(\ a^-, -a^-,\ b^-)$	2	$(\ a, -a,\ 0)$	2^+	$(\ a^+, -a^+,\ b^+)$
3^-	$(-a^-, -a^-,\ b^-)$	3	$(-a, -a,\ 0)$	3^+	$(-a^+, -a^+,\ b^+)$
4^-	$(-a^-,\ \ a^-,\ b^-)$	4	$(-a,\ \ a,\ 0)$	4^+	$(-a^+,\ \ a^+,\ b^+)$

The spherical symmetry of the space must impose some restrictions on the curvature components in the Riemann normal coordinates. Recall that the general form of a RNC metric is

$$g_{\mu\nu}(x) = g_{\mu\nu} - \frac{1}{3}R_{\mu\alpha\nu\beta}\, x^\alpha x^\beta + \mathcal{O}(\epsilon^3)$$

The only parameters which we can play with are the $R_{\mu\alpha\nu\beta}$. Thus to respect the required symmetries we must restrict these parameters accordingly. To do this we revert for the moment to a generic spherically symmetric metric

$$ds^2 = dr^2 + \eta(r)^2\left(d\theta^2 + \sin^2\theta\, d\phi^2\right)$$

where $\eta(r)$ is any smooth function and r is the radial proper distance measured from the throat (this was written as l in the previous sections). In these coordinates there are only two non-trivial frame components,

$$\begin{aligned} R_{\hat{r}\hat{\theta}\hat{r}\hat{\theta}} &= R_{\hat{r}\hat{\phi}\hat{r}\hat{\phi}} = -\frac{1}{\eta}\frac{d^2\eta}{dr^2} \\ R_{\hat{\theta}\hat{\phi}\hat{\theta}\hat{\phi}} &= \frac{1}{\eta^2}\left(1 - \left(\frac{d\eta}{dr}\right)^2\right) \end{aligned} \tag{3.1}$$

where, for example, $R_{\hat{\theta}\hat{\phi}\hat{\theta}\hat{\phi}} = R_{\mu\nu\alpha\beta}\, e^\mu_{\hat{\theta}} e^\nu_{\hat{\phi}} e^\alpha_{\hat{\theta}} e^\beta_{\hat{\phi}}$. Thus we expect only two non-trivial curvature components in the RNC frame. If we align the r axis with the z axis then it is easy to see that the corresponding non-trivial RNC components must be R_{xyxy} and $R_{xzxz} = R_{yzyz}$. Thus, the RNC metric can be reduced to just

$$ds^2 = dx^2 + dy^2 + dz^2 - \frac{1}{3}R_x(xdy - ydx)^2 - \frac{1}{3}R_z(xdz - zdx)^2 - \frac{1}{3}R_z(ydz - zdy)^2$$

where $R_x = R_{xyxy}$ and $R_z = R_{xzxz} = R_{yzyz}$. Incidently, for any pair of vectors u^μ and v^μ we have

$$R_{\mu\alpha\nu\beta}\, u^\mu u^\nu v^\alpha v^\beta = R_x(v^x u^y - v^y u^x)^2 + R_z(v^x u^z - v^z u^x)^2 + R_z(v^y u^z - v^z u^y)^2$$

Using this metric and the above choice of coordinates we obtain, from the smooth lattice equations,

$$0 = 3L^2 - 12a^2 + 4R_x a^4 \tag{3.2}$$
$$0 = 3(L^-)^2 - 12(a^-)^2 + 4R_x(a^-)^4 + 4R_z(a^- b^-)^2 \tag{3.3}$$
$$0 = 3(L^+)^2 - 12(a^+)^2 + 4R_x(a^+)^4 + 4R_z(a^+ b^+)^2 \tag{3.4}$$
$$0 = 3(d^-)^2 - 6(a - a^-)^2 - 3(b^-)^2 + 2R_z(ab^-)^2 \tag{3.5}$$
$$0 = 3(d^+)^2 - 6(a - a^+)^2 - 3(b^+)^2 + 2R_z(ab^+)^2 \tag{3.6}$$
$$0 = L^2 \cos\beta + 4R_x a^4 \tag{3.7}$$
$$3Ld^- \cos\alpha^- = 6a(a - a^-) - 4R_x a^3(a - a^-) - 2R_z(ab^-)^2$$
$$3Ld^+ \cos\alpha^+ = 6a(a - a^+) - 4R_x a^3(a - a^+) - 2R_z(ab^+)^2$$

We have previously stated that the radial edges of our tube must be global geodesics. Thus there can be no kink in the incoming and outgoing edges at vertices 1,2,3 and 4. This implies that

$$\alpha^+ + \alpha^- = \pi$$

which using the above leads to

$$\begin{aligned} 0 = \quad & d^+ \left(6a(a - a^-) - 4R_x a^3(a - a^-) - 2R_z(ab^-)^2\right) \\ & + d^- \left(6a(a - a^+) - 4R_x a^3(a - a^+) - 2R_z(ab^+)^2\right) \end{aligned} \tag{3.8}$$

There are seven quantities that we must compute $a, a^+, a^-, b^+, b^-, R_x$ and R_z. We thus need seven equations which we take to be equations (3.2–3.7) and (3.8). Though this may seem like a well defined system with seven equations for seven unknowns there is a serious problem. Suppose we were to freely choose all of the d^+, d^-, L^+, L, L^- and $\cos\beta$. We could then solve the lattice equations and thus obtain the curvatures in each RNC frame along the tube. Since this is a well defined set of equations we see that this is equivalent to having an arbitrarily specified set of curvatures along the tube. However, in the continuum metric the two curvatures are derived from one function and therefore they cannot be freely specified. Indeed from (3.1) we see that

$$0 = \frac{d}{dr}\left(\eta^2 R_{\hat{x}}\right) - \left(\frac{d\eta^2}{dr}\right) R_{\hat{z}} \tag{3.9}$$

where $R_{\hat{x}} = R_{\hat{\theta}\hat{\phi}\hat{\theta}\hat{\phi}}$ and $R_{\hat{z}} = R_{\hat{r}\hat{\theta}\hat{r}\hat{\theta}}$. This is nothing other than the standard Bianchi identity for the continuum metric. We can expect that a similar but discrete version of this equation must also exist in our smooth lattice model.

3.1. Bianchi Identities

It is well known [6] that a necessary and sufficient condition for the existence of a metric $g_{\mu\nu}(x)$ from which a given curvature tensor $R_{\mu\nu\alpha\beta}$ can be derived is just the Bianchi identities

$$0 = R_{\mu\nu\alpha\beta;\rho} + R_{\mu\nu\beta\rho;\alpha} + R_{\mu\nu\rho\alpha;\beta}$$

In each of our RNC frames this can be written as

$$0 = R_{\mu\nu\alpha\beta,\rho} + R_{\mu\nu\beta\rho,\alpha} + R_{\mu\nu\rho\alpha,\beta}$$

since $\Gamma^{\mu}_{\alpha\beta}(x) = \mathcal{O}(\epsilon^2)$ throughout each RNC (in the conformal metric, see the Appendix). Unfortunately we cannot make much use of this equation as it stands. The problem is that the inversion of the smooth lattice equations returns the curvatures but not their derivatives. One might object by arguing that for the RNC metric we can evaluate the curvature and its derivatives to any order. This may be so but such calculations cannot be expected to be accurate estimates of those quantities for the smooth metric (that the lattice is interpolating). The same situation arises in the much simpler case of a piecewise quadratic interpolation of a function of one variable. The third derivatives of each interpolant is zero yet it is most unlikely that the function has a zero third derivative at each point. The normal practice is to use the second derivative of the interpolant as an estimate at just one point, usually at the central point. Estimates of higher derivatives can then be obtained by interpolation of this derived data.

This same philosophy seems appropriate for our lattice. The estimates for the curvatures are valid at just one point, the origin of the RNC. Derivatives of the curvatures should be estimated by differentiation of a local interpolation of the point estimates of the curvatures. There is one slight subtlety here – the curvatures are defined in different RNC frames. This will require some coordinate transformations to bring the local curvatures into one common frame before the interpolation and differentiation can be performed. This is actually not very difficult. Suppose for example that the origins of two neighbouring frames are O and O'. Suppose that the associated metric and curvatures are $g_{\mu\nu}, R_{\mu\nu\alpha\beta}$ and $g_{\mu'\nu'}, R_{\mu'\nu'\alpha'\beta'}$ respectively. We seek the representation of $R_{\mu'\nu'\alpha'\beta'}$ in the RNC at O. To do this start with the set of coordinate basis vectors at O' and parallel transport them to O. They will be related to the basis vectors at O by some transformation matrix $\Lambda^{\mu'}{}_{\nu}$. Then the transformed value of the curvature will be $R_{\mu'\nu'\alpha'\beta'}\Lambda^{\mu'}{}_{\mu}\Lambda^{\nu'}{}_{\nu}\Lambda^{\alpha'}{}_{\alpha}\Lambda^{\beta'}{}_{\beta}$. For this calculation we can, to leading order in ϵ, evaluate $\Lambda^{\mu'}{}_{\nu}$ solely from the flat space parts of the metrics $g_{\mu\nu}$ and $g_{\mu'\nu'}$.

Though the procedure just described may be suitable for a generic lattice there is a simpler approach for our symmetric lattice. The idea is to use the equivalent integral representation

of the Bianchi identities. In three dimensions this happens to be

$$\begin{aligned} 0 &= \int_M \left(R_{\mu\nu\alpha\beta,\rho} + R_{\mu\nu\beta\rho,\alpha} + R_{\mu\nu\rho\alpha,\beta} \right) \, dx^\alpha dx^\beta dx^\rho \\ &= \int_{\partial M} R_{\mu\nu\alpha\beta} \, dx^\alpha dx^\beta \end{aligned}$$

where M is an arbitrary three dimensional region with boundary ∂M. To leading order in ϵ the limits of integration can be set as if M was everywhere flat. This later form is much easy to apply since it does not require estimates of the derivatives of the curvatures. For our lattice we will choose M to be the pair of cells that define the typical RNC frame. Though this consists of two cells and thus ten boundary faces we can treat them, to leading order in ϵ, as just one larger cell (ie. a linear cell, with six faces, that expands from L^- to L^+ over a length $d^- + d^+$). The above equation can then be written as

$$\begin{aligned} 0 = & \int_{S_x^-} R_{\mu\nu\alpha\beta} \, dx^\alpha dx^\beta + \int_{S_x^+} R_{\mu\nu\alpha\beta} \, dx^\alpha dx^\beta \\ & + \int_{S_y^-} R_{\mu\nu\alpha\beta} \, dx^\alpha dx^\beta + \int_{S_y^+} R_{\mu\nu\alpha\beta} \, dx^\alpha dx^\beta \\ & + \int_{S_z^-} R_{\mu\nu\alpha\beta} \, dx^\alpha dx^\beta + \int_{S_z^+} R_{\mu\nu\alpha\beta} \, dx^\alpha dx^\beta \end{aligned}$$

where S_x^-, S_x^+ are the faces of the cells on the $+x$ and $-x$ axes respectively (with similar definitions for the remaining four faces). We will now compute the curvatures on each of these faces in this RNC frame. This information can be obtained by an interpolation and coordinate transformation of the curvatures from neighbouring cells.

At this point, it is appropriate to represent all of the curvature tensors in bivector form. Let $U_{\mu\nu}, V_{\mu\nu}$ and $W_{\mu\nu}$ be an orthonormal set of normalised bivectors ($1 = U_{\mu\nu}U^{\mu\nu}$, $0 = U_{\mu\nu}V^{\mu\nu}$ etc.) associated with the xy, xz and yz planes respectively. Then the curvature tensor at O is

$$R_{\mu\nu\alpha\beta} = R_x U_{\mu\nu} U_{\alpha\beta} + R_z V_{\mu\nu} V_{\alpha\beta} + R_z W_{\mu\nu} W_{\alpha\beta}$$

while at O_z^+ we would have, in the coordinates for O_z^+,

$$R^+_{\mu\nu\alpha\beta} = R^+_x U^+_{\mu\nu} U^+_{\alpha\beta} + R^+_z V^+_{\mu\nu} V^+_{\alpha\beta} + R^+_z W^+_{\mu\nu} W^+_{\alpha\beta}$$

However, it is clear that, to first order in ϵ, the transformation matrix $\Lambda^{\mu'}{}_{\nu}$ for these two frames is just the identity matrix. Thus the linear interpolant for the curvature, along the z

axis between O and O_z^+ is

$$\begin{aligned} R_{\mu\nu\alpha\beta}(d) &= \left(\frac{d}{d^+}\right) R^+_{\mu\nu\alpha\beta} + \left(1 - \frac{d}{d^+}\right) R_{\mu\nu\alpha\beta} \\ &= \left(\left(\frac{d}{d^+}\right) R^+_x + \left(1 - \frac{d}{d^+}\right) R_x\right) U_{\mu\nu}U_{\alpha\beta} \\ &+ \left(\left(\frac{d}{d^+}\right) R^+_z + \left(1 - \frac{d}{d^+}\right) R_z\right) V_{\mu\nu}V_{\alpha\beta} \\ &+ \left(\left(\frac{d}{d^+}\right) R^+_z + \left(1 - \frac{d}{d^+}\right) R_z\right) W_{\mu\nu}W_{\alpha\beta} \end{aligned}$$

where d is the proper distance measured along the z axis from $z = 0$. For the face S_z^+ we have $d = d^+$.

For the interpolation between O and O_x^+, the procedure is much the same with the exception that the transformation matrix $\Lambda^{\mu'}{}_{\nu}$ is now a rotation. Indeed it is easy to see that the bivectors in the two frames are related by

$$\begin{aligned} U^x_{\mu\nu} &= U_{\mu\nu}\cos\Delta\rho + W_{\mu\nu}\sin\Delta\rho \\ V^x_{\mu\nu} &= V_{\mu\nu} \\ W^x_{\mu\nu} &= W_{\mu\nu}\cos\Delta\rho - U_{\mu\nu}\sin\Delta\rho \end{aligned}$$

where $2\sin(\Delta\rho/2) = (L^+ - L^-)/(d^+ + d^-)$. The interpolation can then be obtained by generalising these equations to be active transformations of the original bivectors U, V and W into a moving set of bivectors, namely

$$\begin{aligned} U^x_{\mu\nu}(\rho) &= U_{\mu\nu}\cos\rho + W_{\mu\nu}\sin\rho \\ V^x_{\mu\nu}(\rho) &= V_{\mu\nu} \\ W^x_{\mu\nu}(\rho) &= W_{\mu\nu}\cos\rho - U_{\mu\nu}\sin\rho \end{aligned}$$

leading to

$$R_{\mu\nu\alpha\beta}(\rho) = R_x U^x_{\mu\nu}(\rho)U^x_{\alpha\beta}(\rho) + R_z V^x_{\mu\nu}(\rho)V^x_{\alpha\beta}(\rho) + R_z W^x_{\mu\nu}(\rho)W^x_{\alpha\beta}(\rho)$$

The interpolation to the face S_x^+ can now be obtained by setting $\rho = \Delta\rho/2$. Note that we can use the approximation $\Delta\rho/2 \approx \sin(\Delta\rho/2)$ since the four radial geodesic edges of the tube must be close in order for the smooth lattice to be a good approximation to the smooth continuum metric.

Similar interpolations can be constructed for the remaining faces. These can then be substituted into the Bianchi identity with the result, assuming each $R_{\mu\nu\alpha\beta}$ is constant on each

face,

$$\begin{aligned} 0 = \quad & \left(R_x^+ A_z^+ - R_x^- A_z^-\right) U_{\mu\nu} \\ & + R_z A_x^+ \left(V_{\mu\nu}^y(+\Delta\rho/2) + W_{\mu\nu}^x(+\Delta\rho/2)\right) - R_z A_x^- \left(V_{\mu\nu}^y(-\Delta\rho/2) + W_{\mu\nu}^x(-\Delta\rho/2)\right) \end{aligned}$$

where A_z^+, A_z^- and A_x^+, A_x^- are the areas of S_z^+, S_z^- and S_x^+ respectively. The areas are easily seen to be

$$\begin{aligned} A_z^+ &= \left(L^+\right)^2 \\ A_z^- &= \left(L^-\right)^2 \\ A_x^+ = A_x^- &= \frac{1}{2}\left(L^+ + L^-\right)\left(d^+ + d^-\right) \end{aligned}$$

Contracting the above equation with $U_{\mu\nu}$ and using $\Delta\rho = (L^+ - L^-)/(d^+ + d^-)$ leads directly to

$$0 = \left(L^2 R_x\right)^+ - \left(L^2 R_x\right)^- - \left(L^+ + L^-\right)\left(L^+ - L^-\right) R_z$$

This is our discrete version of the Bianchi identity. It clearly resembles the previous Bianchi identity (3.9) when expressed in finite difference form. Note that contractions with the other bivectors, V and W, leads only to trivial equations.

3.2. The smooth lattice equations

Its been a rather long road but we can now write down all of the smooth lattice equations, namely,

$$0 = 12a^2 - 4R_x a^4 - 3L^2 \tag{3.2.1}$$

$$0 = 12(a^-)^2 - 4R_x(a^-)^4 - 4R_z(a^- b^-)^2 - 3(L^-)^2 \tag{3.2.2}$$

$$0 = 12(a^+)^2 - 4R_x(a^+)^4 - 4R_z(a^+ b^+)^2 - 3(L^+)^2 \tag{3.2.3}$$

$$0 = 6(a - a^-)^2 + 3(b^-)^2 - 2R_z(ab^-)^2 - 3(d^-)^2 \tag{3.2.4}$$

$$0 = 6(a - a^+)^2 + 3(b^+)^2 - 2R_z(ab^+)^2 - 3(d^+)^2 \tag{3.2.5}$$

$$0 = 4R_x a^4 + L^2\cos\beta \tag{3.2.6}$$

$$\begin{aligned} 0 = \quad & d^+\left(6a(a - a^-) - 4R_x a^3(a - a^-) - 2R_z(ab^-)^2\right) \\ & + d^-\left(6a(a - a^+) - 4R_x a^3(a - a^+) - 2R_z(ab^+)^2\right) \end{aligned} \tag{3.2.7}$$

$$0 = R_x + 2R_z \tag{3.2.8}$$

$$0 = \left(L^2 R_x\right)^+ - \left(L^2 R_x\right)^- - \left(L^+ + L^-\right)\left(L^+ - L^-\right) R_z \tag{3.2.9}$$

The second last equation is just the Hamiltonian constraint ${}^{(3)}R = 0$.

3.3. Solution strategy

The smooth lattice was constructed by starting from the throat and successively adding cells to the end of the tube. There are two parts to this scheme, first the choice of initial data at the throat and second, the repeated solution of the smooth lattice equations.

Consider first the generic step in which one extra cell is added to the tube. Suppose we are given values for R_x^- and R_x (from previous calculations). Then we can solve the nine equations (3.2.1–3.2.9) for the nine quantities $a, a^+, a^-, b^+, b^-, R_z, R_x^+, (L^+)^2$ and $\cos\beta$. Then the R_x^- and R_x of the next RNC frame can be taken to be R_x and R_x^+ of the current RNC frame (the transformation matrix between the pair of frames is just the identity matrix, to first order in ϵ). This process can then be repeated as many times as might be required.

All of the equations were solved using a Newton-Raphson method with initial guesses chosen to be flat space. That is, given d^-, d^+, L^- and L, all of the parameters were estimated using $R_x = R_z = 0$. This is very easy to do, leading to

$$\cos\beta = 0$$

$$L^+ = L + \left(\frac{d^+}{d^-}\right)\left(L - L^-\right)$$

$$a = \frac{1}{2}L\,, \qquad a^- = \frac{1}{2}L^-\,, \qquad a^+ = \frac{1}{2}L^+$$

$$b^- = -\left(\left(d^-\right)^2 - \frac{1}{2}\left(L^- - L\right)^2\right)^{(1/2)}$$

$$b^+ = +\left(\left(d^+\right)^2 - \frac{1}{2}\left(L^+ - L\right)^2\right)^{(1/2)}$$

At the throat we need to make a few minor alterations to the above. Our boundary condition is that the throat must be a minimal surface. This constraint can be imposed via a standard reflection symmetric condition. That is, for the RNC centred on a point on the throat we demand that cells on either side of the throat be mirror images of each other. This leads to

$$0 = a^+ - a^- \qquad (3.2.2')$$

$$0 = b^+ + b^- \qquad (3.2.4')$$

and

$$L^+ = L^-$$

$$d^+ = d^-$$

This however leads immediately to a problem with the Bianchi identity at the throat in that it cannot be solved for a unique value for R_x^+. There are two solutions to this problem. First,

one can set

$$0 = R_x^{+} - R_x \tag{3.3.1}$$

This follows from the observation that in the continuum limit, as $d^{+} \to 0$ and $d^{-} \to 0$, the Bianchi identity can be reduced to

$$0 = \frac{d}{dl}\left(L^2 R_x\right) - \left(\frac{dL^2}{dl}\right) R_z$$

which, with $0 = dL/dl$ at the throat, leads to $0 = dR_x/dl$ and hence the estimate $R_x^{+} = R_x$.

The second solution is to combine the above the differential equation with the constraint $0 = R_x + 2R_z$. This leads directly to

$$0 = \frac{d}{dl}\left(L^3 R_x\right)$$

and thus

$$0 = \left(L^3 R_x\right)^{+} - \left(L^3 R_x\right) \tag{3.3.2}$$

Though this is valid along the whole tube we only apply it at the throat so as not to compromise the independence of the smooth lattice equations (we want the method to stand on its own and not to be supported or dragged along by results from the continuum).

At the throat we replaced the equations (3.2.2,3.2.4) and (3.2.9) with the equations (3.2.2′, 3.2.4′) and (3.3.2). The nine equations were then solved for the same nine quantities using as initial guesses

$$\cos\beta = 0$$

$$L^{-} = L^{+} = L$$

$$a^{-} = a = a^{+} = \frac{1}{2}L$$

$$-b^{-} = b^{+} = d^{+}$$

$$R_x = R_z = 0$$

Using these initial guesses, the Newton-Raphson method for both the generic and initial problems converged in less then five iterations.

Now let us return to the first point raised at the beginning of this section, namely, the choice of initial data L, L^{+} and R_x on the throat. Collectively this corresponds to setting the ADM mass and the fraction of a 2-sphere covered by each tile (such as $(1, 2, 3, 4)$ in Figure (8)). These could be chosen randomly but instead we chose to compute them from the known 3-metric so that we could explore the convergence properties of the smooth lattice solutions.

Indeed the easiest way to compare the smooth lattice solutions against the exact 3-metric is to mimic the construction of the lattice using the exact 3-metric. Thus we construct a series of concentric 2-spheres and four radial geodesics. The vertices of the lattice arise as the intersections of the radial geodesics with the 2-spheres. All of the leg lengths, angles and curvatures can then be computed and compared with those from the smooth lattice.

The exact metric in isotropic coordinates is

$$ds^2 = \rho(r)^4 \left(dr^2 + r^2(d\theta^2 + \sin^2\theta\, d\phi^2)\right) \tag{3.3.3}$$

where $\rho(r) = 1 + m/(2r)$. For all of our calculations we chose $m = 1$.

We chose the coordinates of the vertices according to the following table.

Table 3. Coordinates for the vertices of the exact lattice.

Vertex	(r, θ, ϕ)	**Vertex**	(r, θ, ϕ)	**Vertex**	(r, θ, ϕ)
1^-	$(r^-, \Delta\theta, 0)$	1	$(r, \Delta\theta, 0)$	1^+	$(r^+, \Delta\theta, 0)$
2^-	$(r^-, \Delta\theta, \pi/2)$	2	$(r, \Delta\theta, \pi/2)$	2^+	$(r^+, \Delta\theta, \pi/2)$
3^-	$(r^-, \Delta\theta, \pi)$	3	$(r, \Delta\theta, \pi)$	3^+	$(r^+, \Delta\theta, \pi)$
4^-	$(r^-, \Delta\theta, 3\pi/2)$	4	$(r, \Delta\theta, 3\pi/2)$	4^+	$(r^+, \Delta\theta, 3\pi/2)$

The size of the patch on the initial 2-sphere is determined by the value of $\Delta\theta$. We chose $\Delta\theta = \epsilon(\pi/40)$ where ϵ is a scale parameter in the range $1/256 \le \epsilon \le 2$. The effective number of tiles on each 2-sphere can be estimated as $N = 4\pi/(\Delta\theta)^2$ which for the chosen range, corresponds to $509 < N < 134 \times 10^6$ tiles.

The values of r^+ are obtained by solving, via a Newton-Raphson method, the equation

$$\begin{aligned} d^+ &= \int_r^{r^+} \left(1 + \frac{m}{2u}\right)^2 du \\ &= F(r^+) - F(r) \end{aligned} \tag{3.3.4}$$

where $F(u) = u + m\log(2u/m) - m^2/(4u)$. On the throat we chose $r = m/2$ and r^- so that $d^+ = d^- = F(r) - F(r^-)$.

The exact leg lengths, which we will write as $L^-_\star, L_\star$ and $L^+_\star$, require a little bit of work to compute. They are the lengths of the geodesic segments joining the various vertices. This entails the solution of a two point boundary value problem

$$\begin{aligned} 0 &= \frac{d^2x^\mu}{d\lambda^2} + \Gamma^\mu_{\alpha\beta}(x)\frac{dx^\alpha}{d\lambda}\frac{dx^\beta}{d\lambda} \\ x^\mu(0) &= x^\mu_a\,, \qquad\qquad x^\mu(1) = x^\mu_b \end{aligned} \tag{3.3.5}$$

for the geodesics $x^\mu(\lambda)$ for which we used a simple shooting method built on a 4-th order Runge-Kutta routine. The lengths were then computed by evaluating $\int ds$ along the geodesic. This was done by adding one extra differential equation to the Runge-Kutta routine, namely,

$$\frac{dL}{d\lambda} = \left(g_{\mu\nu}(x) \frac{dx^\alpha}{d\lambda} \frac{dx^\beta}{d\lambda} \right)^{(1/2)} \tag{3.3.6}$$

In solving the above two point boundary value problem we used isotropic x, y, z coordinates so as to avoid the coordinate singularity at $\theta = 0$. Though we did not need to integrate through this singularity its presence degrades the quality of our estimates for the geodesics and the leg lengths.

The frame components of the curvature are easily computed from the above metric (3.3.3) with the result that

$$(R_x)_\star \equiv R_{\hat{\alpha}\hat{\beta}\hat{\alpha}\hat{\beta}} = \frac{2m}{r^3 \rho(r)^6} \tag{3.3.7}$$

$$(R_z)_\star \equiv R_{\hat{r}\hat{\alpha}\hat{r}\hat{\alpha}} = R_{\hat{r}\hat{\beta}\hat{r}\hat{\beta}} = \frac{-m}{r^3 \rho(r)^6} \tag{3.3.8}$$

where $\rho(r) = 1 + m/(2r)$.

The above equations (3.3.4–3.3.7) were used to compute initial values for $L_\star, L^+_\star$ and $(R_x)_\star$. These were then assigned to L, L^+ and R_x. The radial leg lengths d^+ were chosen to be $d^+ = \gamma L$ where γ is a fixed constant. This choice ensures that the cells do not become too fat nor too elongated as successive cells are added to the tube. This scheme provides for an adjustable step length, short steps near the throat where the curvatures are large but longer steps away from the throat where the curvatures are weak. In all of our calculations we set $\gamma = 0.1$ which we arrived at by direct experimentation (this point will be discussed further in the following section).

3.4. Results

The smooth lattice equations (3.2.1–3.2.9) were repeatedly solved to generate data out to $l = 50$. As each new cell of the lattice was constructed, the equation (3.3.4) was solved so that the smooth lattice quantities L, R_x and R_z could be compared with the exact values $L_\star, (R_x)_\star$ and $(R_z)_\star$.

The errors between the exact and smooth lattices depend upon the distance along the edge of the tube measured from the throat $l = \sum d^+$ and upon the choice of $\Delta\theta$. The fractional

errors were computed as

$$EL(l,\epsilon) = -1 + \frac{L}{L_\star}$$
$$ER_x(l,\epsilon) = -1 + \frac{R_x}{(R_x)_\star}$$
$$ER_z(l,\epsilon) = -1 + \frac{R_z}{(R_z)_\star}$$

where $\epsilon = (40/\pi)\Delta\theta$ is the scale parameter. These errors are displayed in Figure (9) and clearly show that the errors vanish, at fixed l, as $\Delta\theta \to 0$. However, for a fixed $\Delta\theta$, the errors appear to grow without bound for increasing values of l. This is much like the behaviour we encountered in section (2.3) (though much less pronounced). We can infer from that section that the divergence in the errors in this example may also be due to an ambiguity in correlating the radial positions between the numerical and exact metrics. For our smooth lattice there are at least two ways to measure the radial proper distance. One can measure it along the outer edges of the tube, as we have done, or along the central geodesic (ie. along the z axis). It is an arbitrary choice as to which of these is to be used to define a radial position in the exact metric. Both choices agree at the throat but progressively diverge as we move away from the throat (because the tube is always increasing in cross section).

We have also estimated the rate of convergence by plotting the errors as function of ϵ for a series of fixed values of l. These are displayed in Figure (10) and clearly show that the convergence of each of the quantities, L, R_x, R_z to their continuum values is quadratic in the lattice spacing. The wiggles in the lower left corner are probably due to round-off errors becoming significant.

3.5. Variations

Three variants of the above smooth lattice method were tried. First we repeated the above calculations but this time using equation (3.3.1) instead of (3.3.2) as our boundary condition on the throat. The results are plotted in Figures (11,12) and the only significant difference is the appearance of an instability in the errors of the curvatures. The amplitude and wavelength of the oscillations in the curvatures were both found to decrease with decreasing γ. For $\gamma \approx 2$ the errors peaked at about 40 (very large indeed!) with only about two cycles occurring. By trial and error we judged $\gamma = 0.1$ to give the most pleasing results (to the eye). Note also that in the regions where the *relative errors* ER_x are large and oscillatory, the *absolute errors* $R_x - (R_x)_\star$ are of order 10^{-5}. Thus this instability is not a cause for great concern. Indeed it appears to have little effect on the errors in the leg lengths (compare Figures (9) and (11)).

For our second variation we took advantage of the integrated form of the Bianchi identity (3.3.2) to replace the smooth lattice equation (3.2.9) with the equation

$$k = L^3 R_x \qquad (3.2.9')$$

with k a constant computed on the throat from the exact metric. The nine equations $(3.2.1 - 3.2.8)$ and $(3.2.9')$ were solved for the nine quantities $a, a^+, a^-, b^+, b^-, R_z, R_x, (L^+)^2$ and $\cos\beta$. The results for this variation were much the same as for the original method. However, this variation showed no signs of instability in the errors in the curvatures.

Our third and final variation was designed so as to remove the need for the Bianchi identities. Recall that the Bianchi identity was required to constrain the two degrees of freedom in the curvatures R_x and R_z so that they were derivable from one metric function. We know that in the exact metric each tile such as $(1, 2, 3, 4)$, *when viewed as a tile on the 2-sphere*, is a scaled image of the tile on the throat. It is not unreasonable to expect that when the tiles are built with respect to the full 3-metric a similar though approximate scaling could be used and that the associated errors would be negligible for small tiles. To investigate this opinion we altered the structure of the lattice to include a diagonal brace joining vertices 1 to 3. Similar braces were also included for the pairs of vertices $1^-, 3^-$ and $1^+, 3^+$. The lengths of these diagonals will be denoted by m, m^- and m^+ respectively. The $\cos\beta$'s are discarded in favour of these diagonals. It is a straightforward calculation, from the main smooth lattice equations (1.2), to show that

$$0 = 8a^2 - m^2 \tag{3.5.1}$$

The condition that each tile is a scaled version of the tile on the throat can be written as

$$0 = L^2 - (k'm)^2 \tag{3.5.2}$$

where k' is constant along the tube. There are two apparently reasonable choices for the constant k'. It could be calculated either from the exact 3-metric on the throat or from the distant regions, far from the throat, where the metric is flat. In fact both choices are unacceptable. The former choice, setting k' on the throat, cannot be used because it does not allow the lattice (with our assumed coordinates, see Table (2)) to become asymptoticly flat. For smaller and smaller sizes of the initial tile on the throat we can expect that the asymptotic curvature might also get smaller and smaller yet it seems unlikely that this could save the day. In the second choice, which requires $(k')^2 = 1/2$, we find by direct inspection of the smooth lattice equations that $0 = R_x = R_z$ everywhere (which when coupled with the boundary condition on the throat then forces $L^- = L = L^+$ along the tube). Thus this second choice certainly cannot be used. We thus opted for the first choice (but with few expectations).

In a typical RNC we computed, for this variation, $a, a^+, a^-, b^+, b^-, R_z, R_x, (L^+)^2$ and m^2. This required nine equations which we took to be the smooth lattice equations (3.2.1–3.2.9) with (3.2.6), which defines $\cos\beta$, and (3.2.9), the Bianchi identity, replaced by (3.5.1) and (3.5.2). The results are displayed in Figure (13) and are as expected – the method does not converge in any sense. It appears that forcing the tiles of the smooth lattice to observe the same symmetries as the tiles of the 2-spheres is incorrect. We conclude that the Bianchi identities cannot be ignored – they are essential in providing the correct constraint on the L's and $\cos\beta$'s (or the L's and m's).

3.6. Are the Bianchi identities essential?

Much has been made of the Bianchi identities and the role that they play in the smooth lattice equations. Yet does it not seem odd that in the smooth lattice approach we find ourselves computing one of the curvatures by integrating a differential equation yet all standard formulas give the curvatures as explicit functions? As another explanation as to why this is so consider the frame components of the curvature of the exact metric. These are

$$(R_z)_\star = -\frac{1}{\eta}\frac{d^2\eta}{dr^2}$$

$$(R_x)_\star = \frac{1}{\eta^2}\left(1 - \left(\frac{d\eta}{dr}\right)^2\right)$$

If we now choose the leg lengths according to $L(r) = \eta(r)\Delta\theta$ then we get

$$(R_z)_\star = -\frac{1}{L}\frac{d^2L}{dr^2}$$

$$(R_x)_\star = \frac{1}{L^2}\left((\Delta\theta)^2 - \left(\frac{dL}{dr}\right)^2\right)$$

Now suppose that all we are given are the discrete leg-lengths and that we wish to extract the curvatures from the discrete lattice. We can expect that in some continuum limit we would recover the above formulae. But where in this process would the number $\Delta\theta$ come into the game? How is it extracted from the discrete lattice (prior to the continuum limit) and how do we know that it is a constant along the tube? The answer must lie partly in the constraint that the radial edges be global geodesics and partly in the use of the Bianchi identities. In fact it is easy to show (see section (4) below) that, in the continuum limit, equations (3.2.1–3.2.7), can be reduced to just

$$R_z = -\frac{1}{L}\frac{d^2L}{dr^2}$$

while from the remaining equations (3.2.8–3.2.9) we can obtain

$$R_x = \frac{1}{L^2}\left(k'' - \left(\frac{dL}{dr}\right)^2\right)$$

where k'' is a constant along the tube. That this constant equals $(\Delta\theta)^2$ can be seen by evaluating this expression for large r where the curvatures vanish. Thus using a metric such as (3.3.3) introduces global information that is simply not accessible from the purely local calculations used in one RNC of the smooth lattice.

This again shows the essential nature of the Bianchi identities in producing the correct estimates for the curvatures.

4. The Continuum Limit

Though the numerical results presented in the previous sections provide strong evidence that the smooth lattice equations are a convergent approximation to the correct differential equations it would be nice to establish this by direct analytical methods.

The most direct route to the continuum is to introduce a scaling for all the leg lengths such as $L \to \epsilon L$, $d^{+} \to \epsilon d^{+}$ etc., and to then express the solutions for $a, a^{+}, \cdots$ as power series in ϵ. The terms in the power series can be obtained by substitution into the smooth lattice equations. From equations (3.2.1–3.2.5) we obtain, assuming R_x and R_z are known,

$$
\begin{aligned}
a &= \frac{L}{2}\left(1 + \frac{1}{24}R_x L^2 + \mathcal{O}(\epsilon^4)\right) \\
a^{+} &= \frac{L^{+}}{2}\left(1 + \frac{1}{24}R_x (L^{+})^2 + \frac{1}{6}R_z\left((d^{+})^2 - \frac{1}{2}(L - L^{+})^2\right) + \mathcal{O}(\epsilon^4)\right) \\
a^{-} &= \frac{L^{-}}{2}\left(1 + \frac{1}{24}R_x (L^{-})^2 + \frac{1}{6}R_z\left((d^{-})^2 - \frac{1}{2}(L - L^{-})^2\right) + \mathcal{O}(\epsilon^4)\right) \\
(b^{+})^2 &= (d^{+})^2 - \frac{1}{2}(L - L^{+})^2 + \mathcal{O}(\epsilon^4) \\
(b^{-})^2 &= (d^{-})^2 - \frac{1}{2}(L - L^{-})^2 + \mathcal{O}(\epsilon^4)
\end{aligned}
$$

The expansions have been carried as far as is necessary to obtain the continuum limit. These can be substituted into equation (3.2.7) which can then be reduced to a differential equation by employing the usual Taylor series expansions

$$
\begin{aligned}
L^{+} &= L + \left(\frac{dL}{dl}\right) d^{+} + \left(\frac{d^2 L}{dl^2}\right) \frac{(d^{+})^2}{2} + \cdots \\
L^{-} &= L - \left(\frac{dL}{dl}\right) d^{-} + \left(\frac{d^2 L}{dl^2}\right) \frac{(d^{-})^2}{2} + \cdots
\end{aligned}
$$

where l is the proper distance measured from the throat. The result, after cancelling a common factor of $-3d^{+}d^{-}(d^{+} + d^{-})L/2$, is

$$
0 = \left(\frac{d^2 L}{dl^2} + R_z L\right) + \mathcal{O}(\epsilon^3) + \mathcal{O}\left((d^{+} - d^{-})^2\right)
$$

The first error term $\mathcal{O}(\epsilon^3)$ arises from the curvature terms in the smooth lattice equations while the second error term $\mathcal{O}\left((d^{+} - d^{-})^2\right)$ arises from the $\mathcal{O}(\epsilon^3)$ terms in the Taylor series expansion in L. Clearly in the limit when $\epsilon \to 0$ we recover the correct differential equation.

We can also see that when the successive d^{+} are chosen to be a smooth function of L then $d^{+} - d^{-} = \mathcal{O}(\epsilon^2)$ and thus the leading error term is $\mathcal{O}(\epsilon^3)$.

Equations (3.2.8–3.2.9) can be treated in a similar fashion leading to

$$0 = \frac{d}{dl}\left(L^2 R_x\right) + \left(\frac{dL^2}{dl}\right) R_z + \mathcal{O}(\epsilon^2)(d^{+} - d^{-})$$

In both of the above equations the errors terms are $\mathcal{O}(\epsilon^2)$ *relative* to the main terms. Thus we can infer that the relative errors $EL(l,\epsilon)$ and $ER_x(l,\epsilon)$ should both be $\mathcal{O}(\epsilon^2)$. This is exactly what we observed in our numerical studies.

We have not used equation (3.2.6) since it can be viewed as a definition of $\cos\beta$.

5. The Regge calculus

The Regge calculus [1] is another lattice theory of General Relativity. Though it employs a lattice it differs significantly from our method in the way in which the field equations are computed from the lattice variables. In the Regge calculus the metric interior to each pair of cells is deemed, a-priori, to be flat. This precludes the use of standard methods for computing the curvatures (such as pointwise differentiation of a metric). Instead one is forced to look at integral quantities, in particular the action integral

$$I = \int R\sqrt{-g}\, d^4x$$

The curvature for the piecewise flat metric can be interpreted in the sense of distributions as a series of Dirac delta functions on the 2-dimensional sub-spaces of the lattice (usually the triangles of a simplicial lattice). The action integral can then be evaluated as

$$I = 2\sum_i \theta_i\, A_i$$

where the sum includes all of the triangles and A_i and θ_i are the areas and defects on these triangles. The Regge field equations are then obtained by extremising the action with respect to the leg lengths, leading to

$$0 = \sum_i \theta_i \frac{\partial A_i}{\partial L_j}$$

There is one such equation for each leg L_j.

Though this derivation mimics that used in Einstein's theory one cannot state, by this fact alone, that the Regge calculus is a consistent discretisation of Einstein's equations. By consistent we mean that as the Regge lattice is successively refined the solutions of the Regge equations converge to solutions of Einstein's equations. Proving this is extremely difficult

primarily because the metric is not differentiable as a point function. Another complication is that any metric can be approximated by many different sequences of lattices yet one would want to develop theorems that account for this vast array of lattices. One firm result has however been proven, [7], that the Regge and Hilbert actions converge when evaluated over a fixed region of the limit smooth space. The proof is very detailed and far from trivial. The state of play is (i) that any smooth metric can be approximated, to any accuracy, by a simplicial metric (such metrics need not be solutions of their equations), (ii) the Regge and Hilbert actions converge when evaluated on a fixed region of the limit smooth space (again, for any smooth metric) but (iii) their remains an open question as to whether or not the limit metric of a sequence of solutions of Regge's equations is also a solution of Einstein's equations.

Of course the later question can be tackled via direct numerical experiments. In all cases reported to date it appears that the Regge solutions do appear to converge to solutions of Einstein's equations. However Brewin [8] has argued that this may be because the experiments have been conducted on highly symmetric spacetimes with the Regge lattices constrained by those symmetries. It could be that the symmetries are so strong as to bring about a concordance between the two theories. Brewin argued that in less symmetric spacetimes the distinction between the two theories may become apparent. He went further to show that even for the symmetric spacetimes, such as Schwarzschild, a lattice that was built purely from 4-simplices and the known exact metric, did not appear to have the appropriate truncation errors when evaluated on the Regge equations. This and other examples were used to argue that the Regge equations might not be a consistent discretisation of Einstein's equations.

In contrast there can be little argument regarding the correct field equations for the smooth lattice approach. They are just the usual Einstein equations.

Of particular note for the current discussion are the calculations of Wong [9]. He used the Regge calculus to solve the time symmetric initial value equations for a Schwarzschild spacetime. He chose two methods, one in which the 2-spheres were triangulated by icosahedra and a second in which he used infinitesimal tiles to generate a rectangular tube similar to our second main example. In this second method Wong proceeded to the limit of vanishingly small cross section in the tube which he called the continuum method. However, in both cases Wong chose to retain a fully discrete radial sub-division. The results for both methods were very good with the typical errors in the range of 1-10% for the icosahedral method and 0.001-1% for the continuum method (for quantities such as volumes and distances from the throat).

It is tempting to compare these results with our own. In the icosahedral method there are 20 triangles per 2-sphere. This lies between the second and third sub-divisions of our first example and to a choice of $\epsilon \approx 10$ in our second example. In both cases we find the error in the leg lengths to be approximately 20% while the errors in the curvatures are approximately 50% for the first example and 100% (yikes!) for the second example. These are larger than

Wong's results which is slightly surprising since fitting a smooth metric to a lattice could be expected to be more accurate than fitting a piecewise flat metric to the same lattice.

Wong's continuum can only be compared with our tube method. We can see from Figure (10) that our errors are around $10^{-5}\%$ whereas Wong's best results are around $10^{-3}\%$. This comparison is a bit unfair on both methods. In all of our calculations the edges of our cells were scaled via the parameter ϵ whereas Wong chose to retain a discrete radial sub-division. This gives an advantage to our method. However where Wong obtains an advantage over our method is in his extensive use of the target continuum metric. Indeed he writes the metric in the form

$$ds^2 = dr^2 + \eta(r)^2 \left(d\theta^2 + \sin^2\theta \, d\phi^2\right)$$

(with a slight change in replacing his $\rho(r)$ with our $\eta(r)$) and estimates all of the leg lengths in the Regge lattice in terms of the unknown function $\eta(r)$ and freely chosen quantities such as $\Delta\theta$ and $\Delta\phi$. In regulating the choice of leg lengths via this metric he has avoided the problem of having too many degrees of freedom in the lattice. We had the same problem but we resolved it by way of the Bianchi identities.

It is unlikely that such a metric ansatz will be available in less symmetric spaces forcing one to look at fully discrete ways in which to impose the desired symmetries. Yet an overly enthusiastic imposition of the symmetries on the space of possible lattices can restrict that space to a set of measure zero. For example, suppose we set out to use the Regge calculus with tubes much like that used in our second example. We could take four such tubes and join them together along one common radial edge. In this model we would not need the $\cos\beta$'s. All of the defects can then be easily calculated. In fact we find that they are **all** non-positive. The only solution of Regge's equations is therefore flat space. This can even be seen without doing any calculations – try fitting the four tubes together in the distant flat regions where the defects should all be close to zero while dL/dr is constant but non-zero. Thus some of the symmetries amongst the legs must be relaxed. But this then introduces extra degrees of freedom. How are they to be constrained? This is where Wong's ansatz saves the day. It allows sufficient variation in the leg lengths of the four tubes so as to obtain meaningful solutions of the Regge equations while retaining the desired spherical symmetries.

It is hard to compare Wong's continuum method and our second example on a level playing field as Wong's method obtains significant advantage in using a method not generally available in a fully discrete implementation of the Regge calculus.

The smooth lattice method could have been applied directly to Wong's icosahedral method. We chose not do so because it seemed unlikely to add anything new to our investigations.

It is important to note that the smooth lattice method uses the same lattice structures as used in the Regge calculus. Thus it inherits all of the attractive features of the Regge calculus, in particular the natural division between the topological and metric information and that the metric is recorded in pure scalar form (eg. the leg lengths). But more importantly, the smooth lattice method has the additional advantage that it extracts a smooth

metric from the lattice and thus that the Einstein equations may be applied directly to the lattice. There is also a practical advantage of the smooth lattice method – the equations are much easier to construct and evaluate than those of the Regge calculus (witness some of the unwieldy calculations of defect angles with their attendant inverse trigonometric and hyperbolic functions, its a mess!). The smooth lattice equations can reasonably be expected to be much quicker to evaluate and to solve on a computer than the Regge equations.

6. Discussion

On the limited evidence provided here it is hard to state with any confidence whether or not the smooth lattice method will be of any use in numerical relativity. However the results are very encouraging. Furthermore the strong theoretical basis for the method, its central use of the equivalence principle and its computational simplicity gives us strong reasons to believe that the method will prove to be useful. Of course much more work needs to be done.

Currently we are adapting these ideas to a 3+1 formulation in which the smooth lattice method is applied to the 3-geometry while retaining a continuous time coordinate. We will employ a dynamical 3-dimensional lattice whose evolution will be controlled by the standard ADM 3+1 equations (which will be applied directly to the 3-lattice). The smooth lattice equations will be used in each time evolution step to aid in the calculation of the source terms. For example, at each time step we would be given a discrete 3-metric on a 3-lattice from which we could estimate the 3-curvatures by way of the smooth lattice equations. There is no role for the Bianchi identities in this phase of the integration, we simply have to live with whatever estimates we get for the curvatures. However we can expect the Bianchi identities to play an important role in the solution of the initial value problem where the initial 3-metric is being constructed. We can speculate that the constraints associated with the Bianchi identities on the 3-metric will be preserved by the 3+1 evolution equations. This is pure speculation at the moment and may in fact prove to be wrong. We will be testing this 3+1 method on the evolution of the Schwarzschild initial data presented here and we hope to report on this work in the near future.

Another interesting question is how much mismatch in the metric do we incur (or how much can we allow) between pairs of adjacent RNC frames? Recall that each RNC frame is constructed by choosing its metric such that it agrees with a finite set of geodesic leg lengths. Consider now two adjacent frames that share a common cell. For a typical curve in that cell this pair of frames will not yield the same estimates for the length of that curve (except on the geodesic edges of that cell). By how much do these estimates differ and is there an optimal choice of curvatures that minimises the difference? If such a minimising relation exists it must constrain the choice of curvatures in each frame. However, we already know that the curvatures must be constrained by the Bianchi identities. How then are these constraints related? This too is currently being investigated.

In both of our examples we chose to solve the Hamiltonian constraint by a radial integration. However the constraints are known to be elliptic equations and so should be properly solved as a boundary value problem. This leads us to an interesting problem. How can asymptotic conditions such as *the conformal factor behaves like* $1 + k/r$ *for large* r be imposed using local Riemann normal coordinates? The difficulty is that this asymptotic condition is a statement about global properties of the space whereas the Riemann normal coordinates are purely local. Another way of looking at this is to ask how can two observers, Joe and Mary, each in their own RNC frame with Mary centred on the throat and Joe in the distant flat regions, determine which observer is in the asymptoticly flat part of the space? Recall that each observer is in a locally freely falling frame and the only geometric quantities that they can measure are the curvature components. Thus the statement that observer Joe is in the asymptoticly flat region must say something about the curvatures measured by Joe relative to those measured by Mary. It would seem that the asymptotic boundary conditions would need to be formulated in terms of the curvatures. Yet such a conclusion seems at odds with the standard theory of elliptic pde's. We seem to be imposing boundary conditions on the *second* derivatives of a function which is a solution of a *second* order elliptic equation. This is indeed odd and needs to be resolved if this method is to be applied to general initial value problems.

7. Appendix

This appendix, which is part of a larger report [5] on Riemann normal coordinates, is included here to provide a self-contained derivation of the two smooth lattice equations (1.2) and (1.3). This will require some preliminary discussion on Riemann normal coordinates. In deriving our equations we will make repeated use of series expansions in the curvature (and its derivatives) around flat space. We have already seen this in action when we wrote the metric as

$$g_{\mu\nu}(x) = g_{\mu\nu} - \frac{1}{3} R_{\mu\alpha\nu\beta}\, x^\alpha x^\beta + \mathcal{O}(\epsilon^3) \tag{1.1}$$

We shall prove this in section (7.3) below.

This expansion can be interpreted as a flat space part plus a (presumably) small quadratic perturbation. Naturally one might have reservations about the convergence of such an expansion. We shall first establish that for sufficiently small regions in which this RNC is defined the truncation errors are negligible. We will do this by introducing a conformal transformation of the original metric. This will prove to be extremely useful. All of the results in this appendix will subsequently be quoted in terms of these conformal coordinates whereas in the body of this paper our results are expressed in the physical coordinates.

For the remainder of this appendix we will be concerned with one RNC frame. We will also refer to the region over which the RNC is defined as the patch (which in the body of the paper consisted of two consecutive cells of the tube or the set of triangles attached to a vertex).

7.1. Conformal coordinates

Let the typical length scale of the patch containing O be ϵ. Let the coordinates of the patch be x^μ and let the coordinates of O be $x^\mu_\star$. Now define a new set of coordinates y^μ by

$$x^\mu = x^\mu_\star + \epsilon y^\mu$$

Then

$$\begin{aligned} ds^2 &= g_{\mu\nu}(x)dx^\mu dx^\nu \\ &= \epsilon^2 g_{\mu\nu}(x_\star + \epsilon y)dy^\mu dy^\nu \end{aligned}$$

Define the conformal metric $d\tilde{s}$ by

$$\begin{aligned} d\tilde{s}^2 &= g_{\mu\nu}(x_\star + \epsilon y)dy^\mu dy^\nu \\ &= \tilde{g}_{\mu\nu}(y,\epsilon)dy^\mu dy^\nu \end{aligned}$$

From the above it is easy to see that, at O,

$$\left.\begin{aligned} \tilde{g}_{\mu\nu} &= g_{\mu\nu} \\ \tilde{g}_{\mu\nu,\alpha} &= \epsilon g_{\mu\nu,\alpha} \\ \tilde{g}_{\mu\nu,\alpha\beta} &= \epsilon^2 g_{\mu\nu,\alpha\beta} \end{aligned}\right\} \tag{7.1.1}$$

where the partial derivatives on the left are with respect to y and those on the right are with respect to x. For each higher derivative an extra power of ϵ will appear.

From the above we immediately obtain

$$\tilde{R}_{\mu\nu\alpha\beta} = \epsilon^2 R_{\mu\nu\alpha\beta}$$

and as $R_{\mu\nu\alpha\beta}$ is independent of ϵ, we see that

$$\tilde{R}_{\mu\nu\alpha\beta} = \mathcal{O}(\epsilon^2)$$

for $\epsilon << 1$.

Clearly, then, as $\epsilon \to 0$ the conformal metric is flat.

There are now two ways to look at the patch. We can view it (in the original coordinates x^μ) as a patch of length scale ϵ with a curvature independent of ϵ. Or we can view it (in the conformal coordinates y^μ) as a patch of fixed size but with a curvature that varies as ϵ^2. This later view is useful since in using it we can be sure that the series expansions around flat space are convergent (for a sufficiently small ϵ).

We will use these conformal coordinates for the remainder of this Appendix. We will also drop the tilde and revert to x^μ as the generic coordinates (even while working in the conformal frame.)

7.2. Riemann normal coordinates

In Riemann normal coordinates the geodesics through O must all be of the form

$$x^\mu(s) = a_1^\mu s$$

for some set of numbers a_1^μ. By direct substitution into the geodesic equation

$$0 = \frac{d^2x^\mu}{ds^2} + \Gamma^\mu_{\alpha\beta}(x)\frac{dx^\alpha}{ds}\frac{dx^\beta}{ds} \tag{7.2.1}$$

and its derivatives, one obtains, at the origin O,

$$0 = \Gamma^\mu_{\alpha\beta} \tag{7.2.2}$$

$$0 = \Gamma^\mu_{\alpha\beta,\nu} + \Gamma^\mu_{\beta\nu,\alpha} + \Gamma^\mu_{\nu\alpha,\beta} \tag{7.2.3}$$

It is easy to see, by continuing in this way, that all symmetric derivatives of the connection vanish at the origin in Riemann normal coordinates.

7.3. Metric

Consider a Taylor series expansion of the metric around the origin O, namely,

$$g_{\mu\nu}(x) = g_{\mu\nu} + g_{\mu\nu,\alpha\beta}\frac{x^\alpha x^\beta}{2} + \mathcal{O}(\epsilon^3)$$

There is no linear term because $g_{\mu\nu,\alpha} = 0$ at the origin. It is a simple algebraic exercise to show, given (7.2.2) and (7.2.3), that

$$\Gamma^\mu_{\alpha\beta,\nu} = -\frac{1}{3}\left(R^\mu{}_{\alpha\beta\nu} + R^\mu{}_{\beta\alpha\nu}\right) \tag{7.3.1}$$

from which it follows that

$$g_{\mu\nu,\alpha\beta} = -\frac{1}{3}\left(R_{\mu\alpha\nu\beta} + R_{\mu\beta\nu\alpha}\right) \tag{7.3.2}$$

and finally

$$R_{\mu\nu\alpha\beta} = g_{\alpha\nu,\mu\beta} - g_{\alpha\mu,\nu\beta}$$

Substituting these into the above we obtain

$$g_{\mu\nu}(x) = g_{\mu\nu} - \frac{1}{3}R_{\mu\alpha\nu\beta}\, x^\alpha x^\beta + \mathcal{O}(\epsilon^3) \tag{1.1}$$

7.4. Connection

We can also propose a Taylor series expansion for the connection about the origin O, namely,

$$\Gamma^{\mu}_{\alpha\beta}(x) = \Gamma^{\mu}_{\alpha\beta} + \Gamma^{\mu}_{\alpha\beta,\rho}x^{\rho} + \Gamma^{\mu}_{\alpha\beta,\rho\tau}\frac{x^{\rho}x^{\tau}}{2} + \cdots$$

Our first observations are that

$$\begin{aligned}\Gamma^{\mu}_{\alpha\beta} &= 0\\ \Gamma^{\mu}_{\alpha\beta,\rho} &= \mathcal{O}(\epsilon^2)\\ \Gamma^{\mu}_{\alpha\beta,\rho\tau} &= \mathcal{O}(\epsilon^3)\end{aligned}$$

and in general the n-th derivative of Γ will be $\mathcal{O}(\epsilon^{n+1})$ at O. This follows by simple inspection of the standard formula for computing the metric connection and the previously stated asymptotic behaviour of the conformal metric (7.1.1).

We are only interested in the leading term in the above expansion, and so after using (7.3.1) we obtain

$$\Gamma^{\mu}_{\alpha\beta}(x) = -\frac{1}{3}\left(R^{\mu}{}_{\alpha\beta\nu} + R^{\mu}{}_{\beta\alpha\nu}\right)x^{\nu} + \mathcal{O}(\epsilon^3) \tag{7.4.1}$$

7.5. Geodesics

For the geodesics, we employ a series expansion in s, the distance measured along the geodesic,

$$x^{\mu}(s) = a^{\mu}_0 + a^{\mu}_1 s + a^{\mu}_2\frac{s^2}{2} + a^{\mu}_3\frac{s^3}{6} + \cdots \tag{7.5.1}$$

We will defer for the moment stating the nature of the truncation error. Our primary aim here is to determine as many of the a^{μ}_i as we can in terms of just $g_{\mu\nu}$ and $R_{\mu\nu\alpha\beta}$. This can be done by demanding that the above expansion for $x^{\mu}(s)$ is a solution of the geodesic equation (7.2.1).

The basic steps are to substitute (7.5.1) into (7.4.1) and to then substitute all of these quantities into the geodesic equation (7.2.1). The result is a polynomial in s and as this must be identically zero for all s, we equate the separate coefficients of powers of s to zero. For the first two terms s^0 and s^1 we obtain, respectively,

$$\begin{aligned}0 &= a^{\mu}_2 + \Gamma^{\mu}_{\alpha\beta,\rho}a^{\rho}_0 a^{\alpha}_1 a^{\beta}_1 + \Gamma^{\mu}_{\alpha\beta,\rho\tau}a^{\rho}_0 a^{\tau}_0 a^{\alpha}_1 a^{\beta}_1\\ 0 &= a^{\mu}_3 + \Gamma^{\mu}_{\alpha\beta,\rho}\left(a^{\rho}_1 a^{\alpha}_1 a^{\beta}_1 + 2a^{\rho}_0 a^{\alpha}_1 a^{\beta}_2\right) + \Gamma^{\mu}_{\alpha\beta,\rho\tau}\left(2a^{\rho}_1 a^{\tau}_0 a^{\alpha}_1 a^{\beta}_1 + 2a^{\rho}_0 a^{\tau}_0 a^{\alpha}_2 a^{\beta}_1\right)\end{aligned}$$

The term $\Gamma^{\mu}_{\alpha\beta,\rho}a^{\rho}_1 a^{\alpha}_1 a^{\beta}_1$ is zero in view of (7.2.3). Thus, to order ϵ^3, we obtain

$$\begin{aligned}a^{\mu}_2 &= -\Gamma^{\mu}_{\alpha\beta,\rho}a^{\rho}_0 a^{\alpha}_1 a^{\beta}_1 + \mathcal{O}(\epsilon^3)\\ a^{\mu}_3 &= \mathcal{O}(\epsilon^3)\end{aligned}$$

Clearly this process can be developed in full to obtain recurrence relations amongst all of the remaining a_i^μ. We will not need these but what we do require is their behaviour in ϵ. It is not hard to see that in the generic equation for a_n^μ the leading terms will be

$$0 = a_n^\mu + \Gamma^\mu_{\alpha\beta,\rho} a_{n-2}^\rho a_1^\alpha a_1^\beta + \cdots$$

Since we have already established that a_2^μ is $\mathcal{O}(\epsilon^2)$ it follows that a_n^μ will be $\mathcal{O}(\epsilon^n)$ for $n \geq 2$.

Assembling the above results leads finally to

$$x^\mu(s) = a_0^\mu + a_1^\mu s + \frac{1}{3} R^\mu{}_{\alpha\beta\rho}\, a_0^\rho a_1^\alpha a_1^\beta s^2 + \mathcal{O}(\epsilon^3) \tag{7.5.2}$$

Notice that a_0^μ and a_1^μ remain undetermined – they can only be computed from appropriate boundary or initial conditions.

7.6. Geodesic boundary value problem

In this case we are looking for the geodesic which passes through two given points. Let the coordinates of initial point be x_i^μ and those for the final point be x_j^μ. Suppose the geodesic distance between the two points is L_{ij}. The L_{ij} cannot be freely specified as they must be derivable from the metric and the coordinates. A equation for L_{ij} will be given in a later section (7.7).

Our aim is to solve for a_0^μ and a_1^μ such that

$$\begin{aligned} x^\mu(s=0) &= x_i^\mu = a_0^\mu + \mathcal{O}(\epsilon^3) \\ x^\mu(s=L_{ij}) &= x_j^\mu = a_0^\mu + a_1^\mu L_{01} + \frac{1}{3} R^\mu{}_{\alpha\beta\rho}\, a_0^\rho a_1^\alpha a_1^\beta L_{01}^2 + \mathcal{O}(\epsilon^3) \end{aligned}$$

The first equation is easy to solve, namely, $a_0^\mu = x_i^\mu + \mathcal{O}(\epsilon^3)$. However, the second equation does appear to pose a bit of a problem – it looks like a nasty quadratic equation for each of the a_1^μ. Fortunately this equation can be solved by an iterative method to within $\mathcal{O}(\epsilon^3)$. The starting point is to first substitute for a_0^μ to obtain

$$x_j^\mu = x_i^\mu + a_1^\mu L_{01} + \frac{1}{3} R^\mu{}_{\alpha\beta\rho}\, x_i^\rho a_1^\alpha a_1^\beta L_{01}^2 + \mathcal{O}(\epsilon^3)$$

We can then re-write this as

$$a_1^\mu = \frac{1}{L_{01}} \left(x_j^\mu - x_i^\mu - \frac{1}{3} R^\mu{}_{\alpha\beta\rho}\, x_i^\rho a_1^\alpha a_1^\beta L_{01}^2 \right) + \mathcal{O}(\epsilon^3)$$

which we will evaluate as a fixed point iteration scheme.

Since $R^{\mu}{}_{\alpha\beta\rho} = \mathcal{O}(\epsilon^2)$ we obtain the first approximation

$$a_1^\mu = \frac{1}{L_{01}}\left(x_j^\mu - x_i^\mu\right) + \mathcal{O}(\epsilon^2)$$

This can now be substituted back into the previous equation leading to the second approximation

$$a_1^\mu = \frac{1}{L_{ij}}\left(\Delta x_{ij}^\mu - \frac{1}{3}R^{\mu}{}_{\alpha\beta\rho}\, x_i^\rho \Delta x_{ij}^\alpha \Delta x_{ij}^\beta\right) + \mathcal{O}(\epsilon^3) \tag{7.6.1}$$

where $\Delta x_{ij}^\mu = x_j^\mu - x_i^\mu$. This is as far as we can proceed with this iteration scheme because the errors in this approximation for a_1^μ and those in the equation we are iterating on are both $\mathcal{O}(\epsilon^3)$. Combining these results for a_0^μ and a_1^μ and substituting into (7.5.2) leads to the following equation for the geodesic passing through the two points x_i^μ and x_j^μ

$$x^\mu(s) = x_i^\mu + \lambda\Delta x_{ij}^\mu - \frac{\lambda(1-\lambda)}{3}R^{\mu}{}_{\alpha\beta\rho}\, x_i^\rho \Delta x_{ij}^\alpha \Delta x_{ij}^\beta + \mathcal{O}(\epsilon^3) \tag{7.6.2}$$

where $\lambda = s/L_{ij}$.

7.7. Geodesic distance

Consider two points with coordinates x_i^μ and x_j^μ. Since there exists, by assumption, a unique geodesic joining this pair of points, the distance between them should also be uniquely defined in terms of their coordinates and the metric.

Our aim is to evaluate, along the geodesic,

$$L_{ij} = \int_0^1 \left(g_{\mu\nu}(x)\frac{dx^\mu}{d\lambda}\frac{dx^\nu}{d\lambda}\right)^{1/2} d\lambda$$

The equation for $x^\mu(\lambda)$ is simply (7.6.2) for $0 < \lambda < 1$. This can be substituted into the expansion (1.1) for $g_{\mu\nu}(x)$ with the result

$$g_{\mu\nu}(x(\lambda)) = g_{\mu\nu} - \frac{1}{3}R_{\mu\alpha\nu\beta}\,\left(x_i^\alpha + \lambda\Delta x_{ij}^\alpha\right)\left(x_i^\beta + \lambda\Delta x_{ij}^\beta\right) + \mathcal{O}(\epsilon^3)$$

It is a simple matter to substitute these into the integrand, leading to

$$\left(\frac{dL}{d\lambda}\right)^2 = g_{\mu\nu}\Delta x_{ij}^\mu \Delta x_{ij}^\nu - \frac{1}{3}R_{\mu\alpha\nu\beta}\, x_i^\alpha x_i^\beta \Delta x_{ij}^\mu \Delta x_{ij}^\nu + \mathcal{O}(\epsilon^3)$$

The important point to note is that this result does not depend on λ. Thus the integrand is constant and so the integration is trivial. The result follows immediately,

$$L_{ij}^2 = g_{\mu\nu}\Delta x_{ij}^\mu \Delta x_{ij}^\nu - \frac{1}{3}R_{\mu\alpha\nu\beta}\, x_i^\alpha x_i^\beta \Delta x_{ij}^\mu \Delta x_{ij}^\nu + \mathcal{O}(\epsilon^3) \tag{7.7.1}$$

From this result it is easy to establish, using the symmetries of $R_{\mu\nu\alpha\beta}$, the following equivalent equations for L_{ij}^2

$$\begin{aligned} L_{ij}^2 &= (g_{\mu\nu} - \frac{1}{3}R_{\mu\alpha\nu\beta}\,\overline{x}_{ij}^{\alpha}\,\overline{x}_{ij}^{\alpha})\Delta x_{ij}^{\mu}\Delta x_{ij}^{\nu} + \mathcal{O}(\epsilon^3) \\ &= g_{\mu\nu}\Delta x_{ij}^{\mu}\Delta x_{ij}^{\nu} - \frac{1}{3}R_{\mu\alpha\nu\beta}\,x_i^{\alpha}x_i^{\beta}x_j^{\mu}x_j^{\nu} + \mathcal{O}(\epsilon^3) \\ &= g_{\mu\nu}\Delta x_{ij}^{\mu}\Delta x_{ij}^{\nu} - \frac{1}{3}R_{\mu\alpha\nu\beta}\,\Delta x_{0i}^{\alpha}\Delta x_{0i}^{\beta}\Delta x_{0j}^{\mu}\Delta x_{0j}^{\nu} + \mathcal{O}(\epsilon^3) \end{aligned} \tag{7.7.2}$$

where $\overline{x}_{ij}^{\mu} = (x_i^{\mu} + x_j^{\mu})/2$ and where x_0^{μ} are the coordinates of the origin (which in our case are zero).

Note that when these equations are re-expressed in terms of the physical metric all that changes is that the error term $\mathcal{O}(\epsilon^3)$ is replaced with $\mathcal{O}(\epsilon^5)$.

7.8. Generalised Cosine law

Consider a geodesic triangle with vertices i, j and k. We would like to be able to compute the angles subtended at each vertex in terms of the usual quantities, the metric, the coordinates etc. We will develop the appropriate equations in two stages. First, we will consider the simple case of computing the angle at a vertex coincident with the origin. We shall then generalise this result to the case were all three vertices are distinct from the origin.

To start the ball rolling consider a geodesic triangle with vertices i, j and O, the origin. We seek an equation for the angle between the geodesic segments joining O to i and O to j. The unit tangent vectors to these geodesic segments at O are, from equation (7.6.2),

$$\begin{aligned} v_{oi}^{\mu} &= \Delta x_{oi}^{\mu}/L_{oi} \\ v_{oj}^{\mu} &= \Delta x_{oj}^{\mu}/L_{oj} \end{aligned}$$

Now let θ_{ij} be the angle subtended at O. Then

$$\cos\theta_{ij} = g_{\mu\nu}v_{oi}^{\mu}v_{oj}^{\nu} = g_{\mu\nu}\Delta x_{oi}^{\mu}\Delta x_{oj}^{\nu}/(L_{oi}L_{oj})$$

We can obtain two useful variants of this equation by writing, first, $\Delta x_{oi}^{\mu} = \Delta x_{oj}^{\mu} - \Delta x_{ij}^{\mu}$ and second, $\Delta x_{oj}^{\mu} = \Delta x_{oi}^{\mu} + \Delta x_{ij}^{\mu}$. This gives

$$\begin{aligned} L_{oi}L_{oj}\cos\theta_{ij} &= g_{\mu\nu}\left(\Delta x_{oj}^{\mu} - \Delta x_{ij}^{\mu}\right)\Delta x_{oj}^{\nu} \\ &= g_{\mu\nu}\Delta x_{oi}^{\mu}\left(\Delta x_{oi}^{\nu} + \Delta x_{ij}^{\nu}\right) \end{aligned}$$

Adding these two equations leads to

$$2L_{oi}L_{oj}\cos\theta_{ij} = L_{oi}^2 + L_{oj}^2 - g_{\mu\nu}\Delta x_{ij}^{\mu}\Delta x_{ij}^{\nu} \tag{7.8.1}$$

However, from equation (7.7.2) we see that

$$g_{\mu\nu}\Delta x^{\mu}_{ij}\Delta x^{\nu}_{ij} = L^2_{ij} + \frac{1}{3}R_{\mu\alpha\nu\beta}\,\Delta x^{\mu}_{oi}\Delta x^{\nu}_{oi}\Delta x^{\alpha}_{oj}\Delta x^{\beta}_{oj} + \mathcal{O}(\epsilon^3)$$

Thus we have

$$2L_{oi}L_{oj}\cos\theta_{ij} = L^2_{oi} + L^2_{oj} - L^2_{ij} - \frac{1}{3}R_{\mu\alpha\nu\beta}\,\Delta x^{\mu}_{oi}\Delta x^{\nu}_{oi}\Delta x^{\alpha}_{oj}\Delta x^{\beta}_{oj} + \mathcal{O}(\epsilon^3) \qquad (7.8.2)$$

With this equation we have achieved our first aim : to obtain an equation when the vertex resides at the origin. To obtain an equation applicable to the general case, where the vertex is not at the origin, we can imagine transforming to a second set of Riemann normal coordinates with an origin at some other point, say O'. We can do this simply by shifting the coordinates, eg. $x^{\mu} \to x^{\mu}+c^{\mu}$. The coordinates, metric and Riemann components at the respective origins will therefore be related by

$$x'^{\mu} = x^{\mu} + c^{\mu}$$

$$g'_{\mu\nu}(O') = g_{\mu\nu}(O) - \frac{1}{3}R_{\mu\alpha\nu\beta}(O)\,c^{\alpha}c^{\beta} + \mathcal{O}(\epsilon^3)$$

$$R'_{\mu\nu\alpha\beta}(O') = R_{\mu\alpha\nu\beta}(O) + \mathcal{O}(\epsilon^1)$$

Now the important observation is that the above equation (7.8.2) is covariant with respect to this transformation (whereas (7.8.1) is not). That is, it applies to any three vertices of a geodesic triangle. Let us now relabel the vertices as i, j and k. Then the angle subtended at vertex k can be computed from

$$2L_{ik}L_{jk}\cos\theta_{ij} = L^2_{ik} + L^2_{jk} - L^2_{ij} - \frac{1}{3}R_{\mu\alpha\nu\beta}\,\Delta x^{\mu}_{ik}\Delta x^{\nu}_{ik}\Delta x^{\alpha}_{jk}\Delta x^{\beta}_{jk} + \mathcal{O}(\epsilon^3) \qquad (7.8.3)$$

As with the geodesic length equation (7.7.1), one need only replace the $\mathcal{O}(\epsilon^3)$ error term with $\mathcal{O}(\epsilon^5)$ to obtain the correct equation in the original physical coordinates.

8. Acknowledgements

I am pleased to acknowledge the many illuminating discussions I have had with Joe Monaghan and Tony Lun on this and many other topics in numerical relativity. I would also like to thank Adrian Gentle and Tony Lun for their careful reading of this paper.

9. References

[**1**] Regge, Tullio. (1961)
General Relativity without Coordinates.
Il Nuovo Cimento. Vol.XIX,No.3(1961) pp.558-571.

[**2**] Petrov, A.Z. (1969)
Einstein Spaces. (Chp.1 sec.7)
Pergamon Press, Oxford. 1969

[**3**] Eisenhart, L.P. (1926)
Riemannian geometry.(Sec.18 and App.3)
Princeton University Press, Princeton 1926

[**4**] Misner, C.W, Thorne, K. and Wheeler, J.A. (1973)
Gravitation (pp.285-287)
W.H. Freeman. San Francisco. 1973.

[**5**] Brewin, L.C. (1997)
Riemann Normal Coordinates.
Department of Mathematics Preprint, Monash University, Clayton, Vic. 3168. Also available from `http://newton.maths.monash.edu.au:8000/papers/rnc-notes.ps.gz`

[**6**] Penrose, R. and Rindler (1984)
Spinors and Spacetime. Vol.1(p.364)
Cambridge University Press. 1984.

[**7**] Cheeger, J, Müller, W and Schrader, R. (1984)
On the Curvature of Piecewise Flat Spaces.
Comm. Math. Phys. Vol.92(1984) pp.405-454.

[**8**] Brewin, L.C. (1995)
Is the Regge Calculus a consistent approximation to General Relativity?
Department of Mathematics Preprint, Monash University, Clayton, Vic. 3168. Also available at `http://newton.maths.monash.edu.au:8000/papers/truncation.ps.gz`

[**9**] Cheuk-Yin Wong (1971)
Application of Regge Calculus to the Schwarzschild and Reisner-Nordstrøm Geometries at the Moment of Time Symmetry.
J.Math.Phys. Vol.12(1971) pp.70-78.

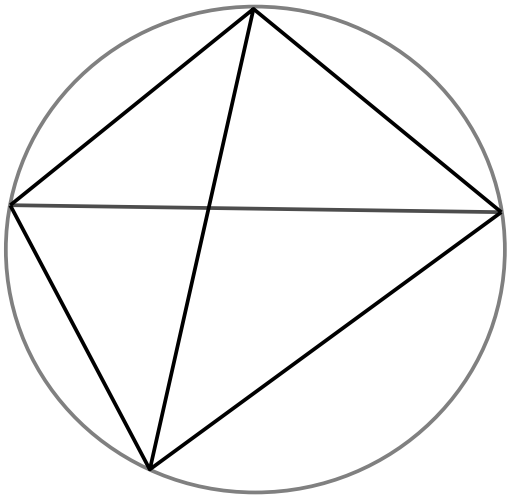

Figure 1 A simple approximation to a 2-sphere. Though the legs of the tetrahedron appear straight they are taken to be geodesic segments of the 2-sphere.

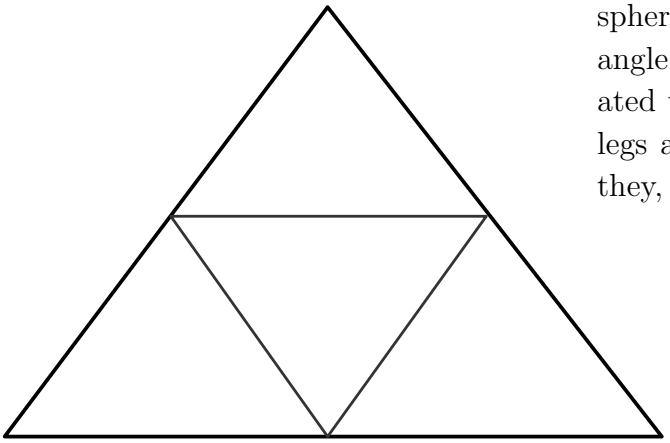

Figure 2 Better approximations for the 2-sphere are obtained by sub-dividing each triangle according to this pattern. Newly created vertices are placed at the centre of old legs and are later displaced radially so that they, the new vertices, touch the 2-sphere.

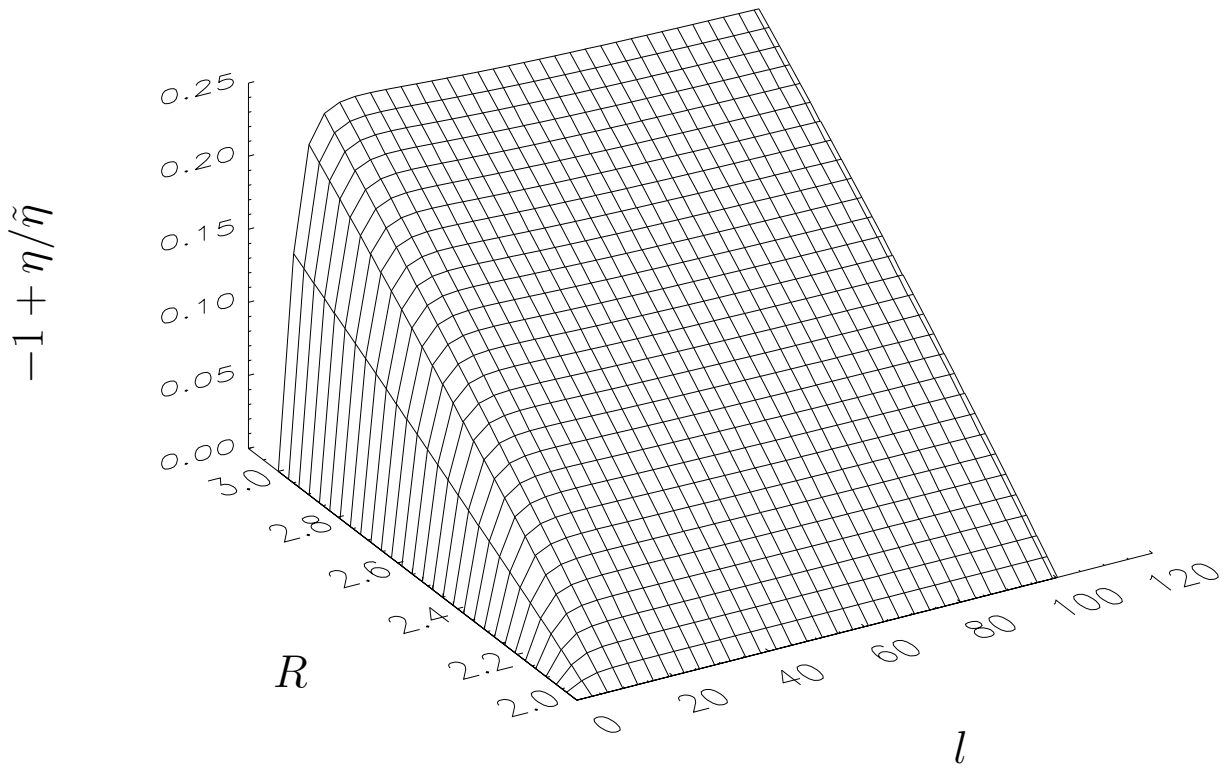

Figure 3 The relative error in η as a function of the distance l from the throat and of the curvature R. Note that the errors vanish as $R \to 2$ while they remain bounded for increasing l.

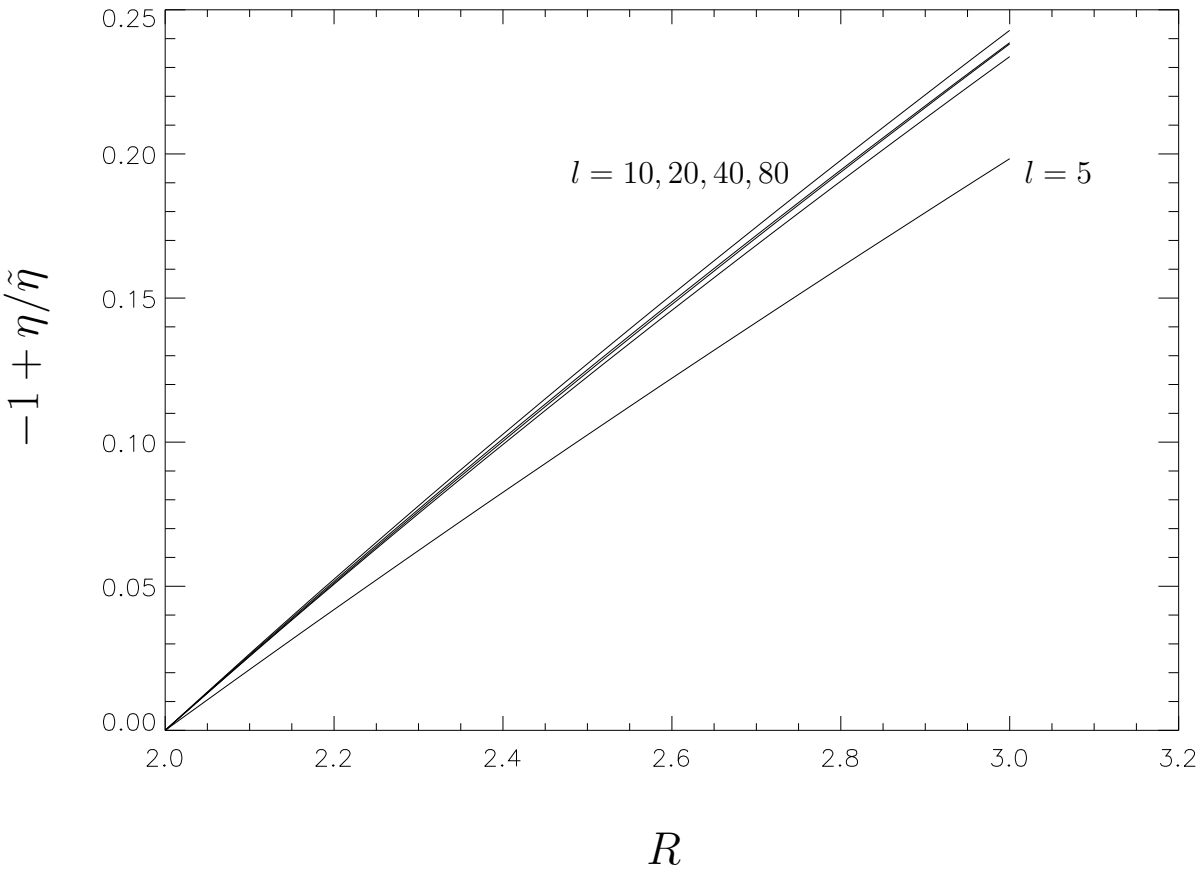

Figure 4 A plot of the relative error in η for various fixed values of l. This plot shows that the error in the metric varies linearly with the error in the curvature.

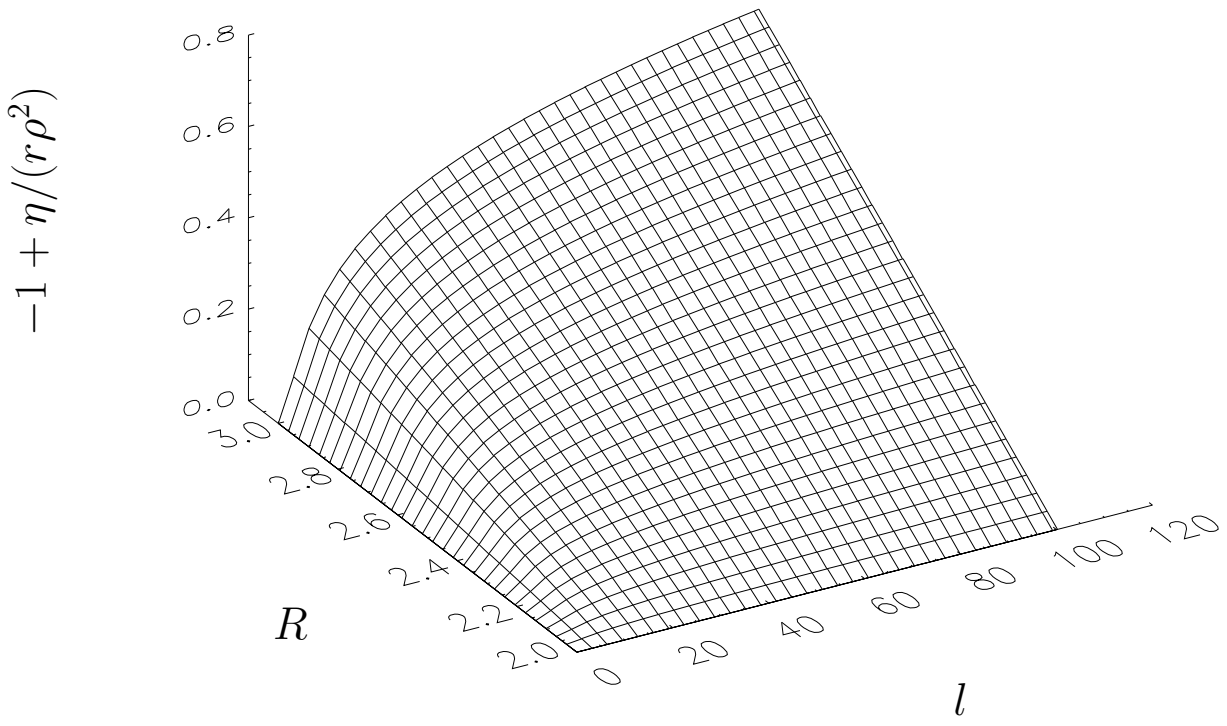

Figure 5 This is similar to Figure (3) but using the alternative definition of the error, equation (2.3.7). Notice that the errors are not bounded for increasing l.

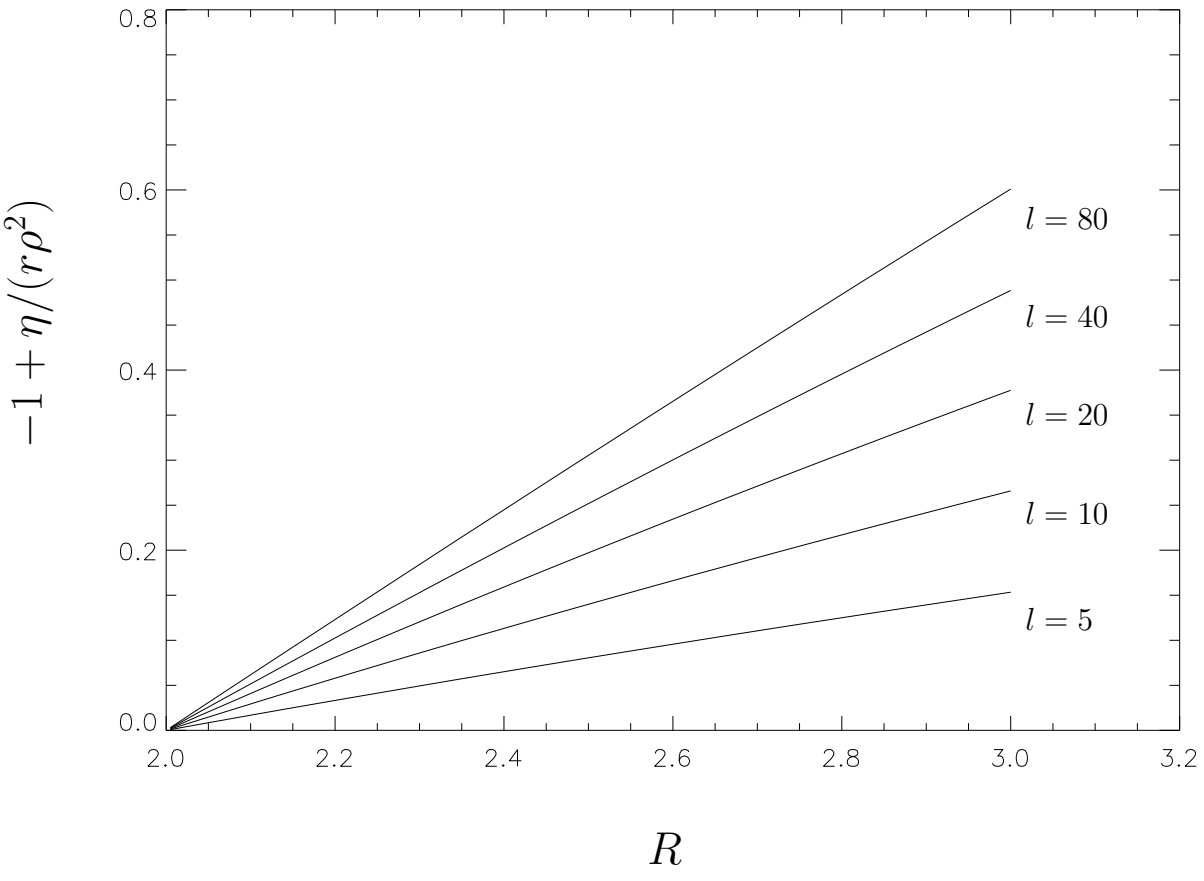

Figure 6 This demonstrates that even though the relative errors in Figure (5) are unbounded for large l, they do vanish as $R \to 2$ at fixed l.

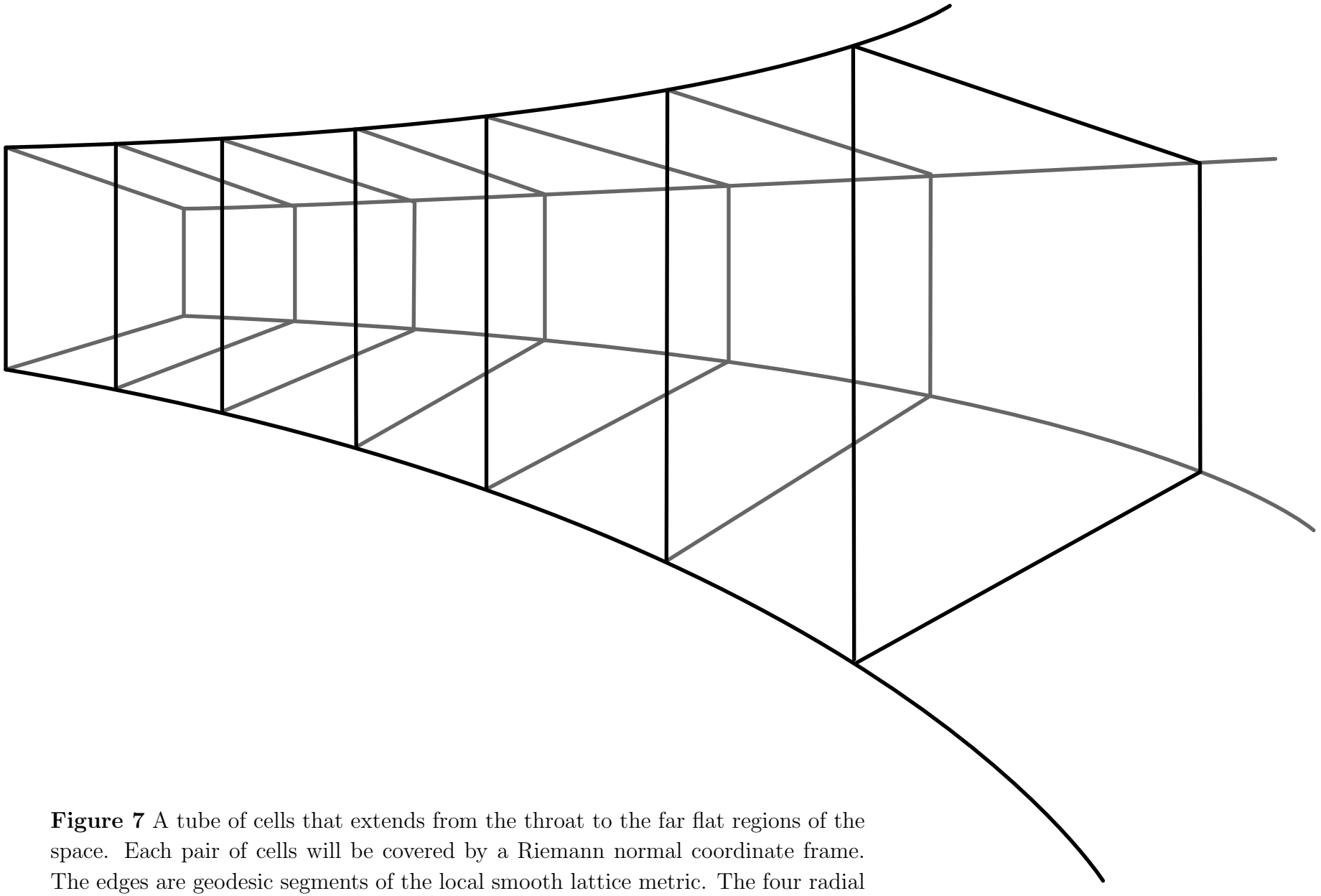

Figure 7 A tube of cells that extends from the throat to the far flat regions of the space. Each pair of cells will be covered by a Riemann normal coordinate frame. The edges are geodesic segments of the local smooth lattice metric. The four radial edges are global geodesics.

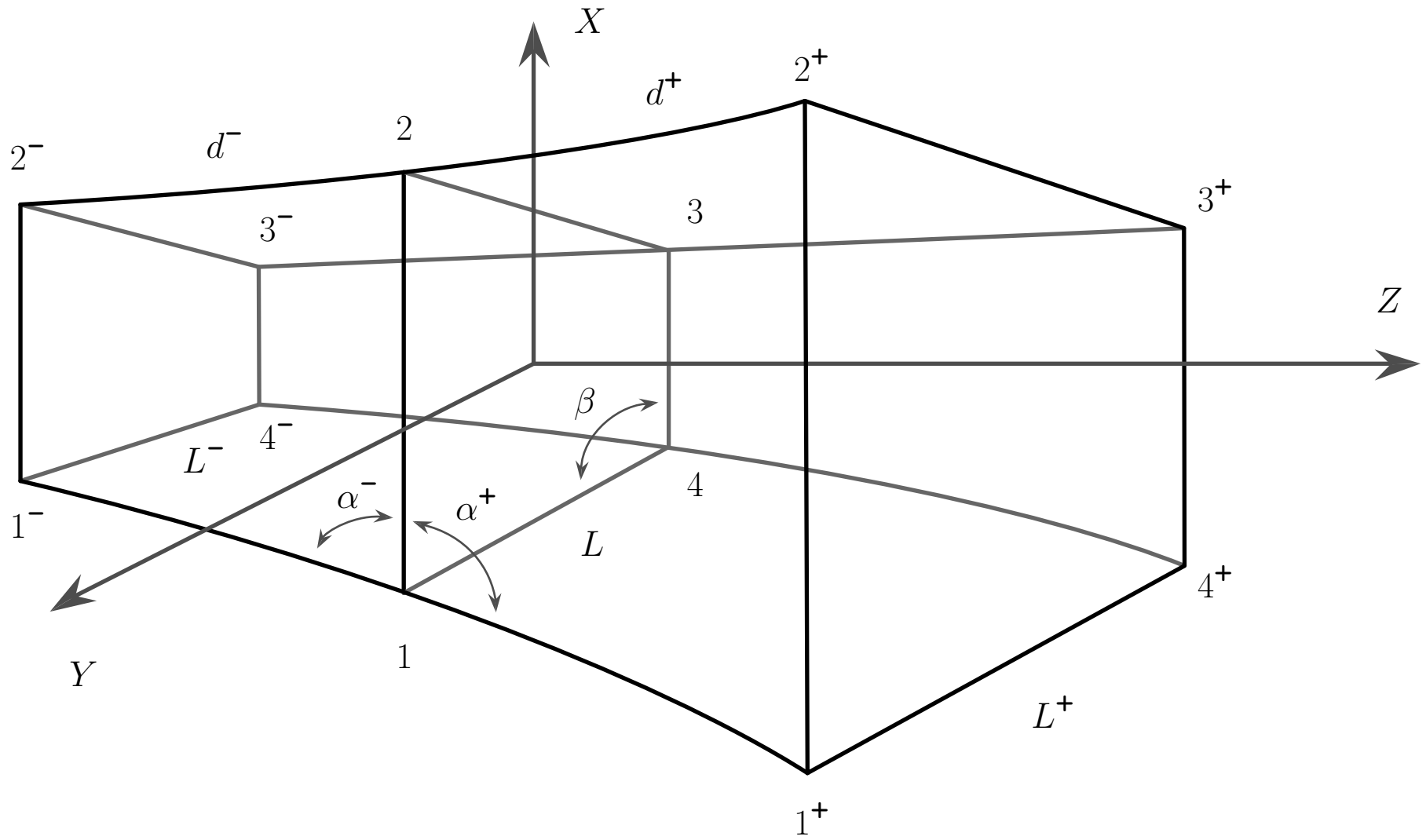

Figure 8 The generic pair of cells for one Riemann normal coordinate frame. The z-axis runs up the middle of the tube.

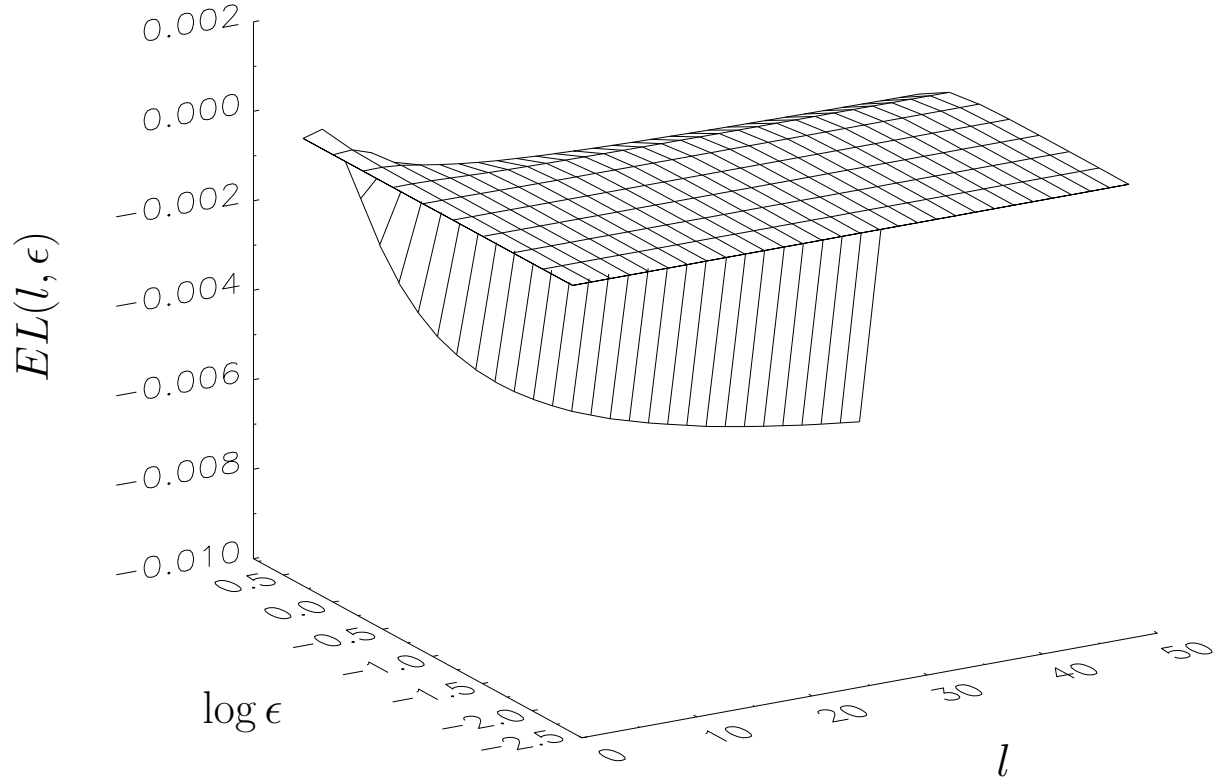

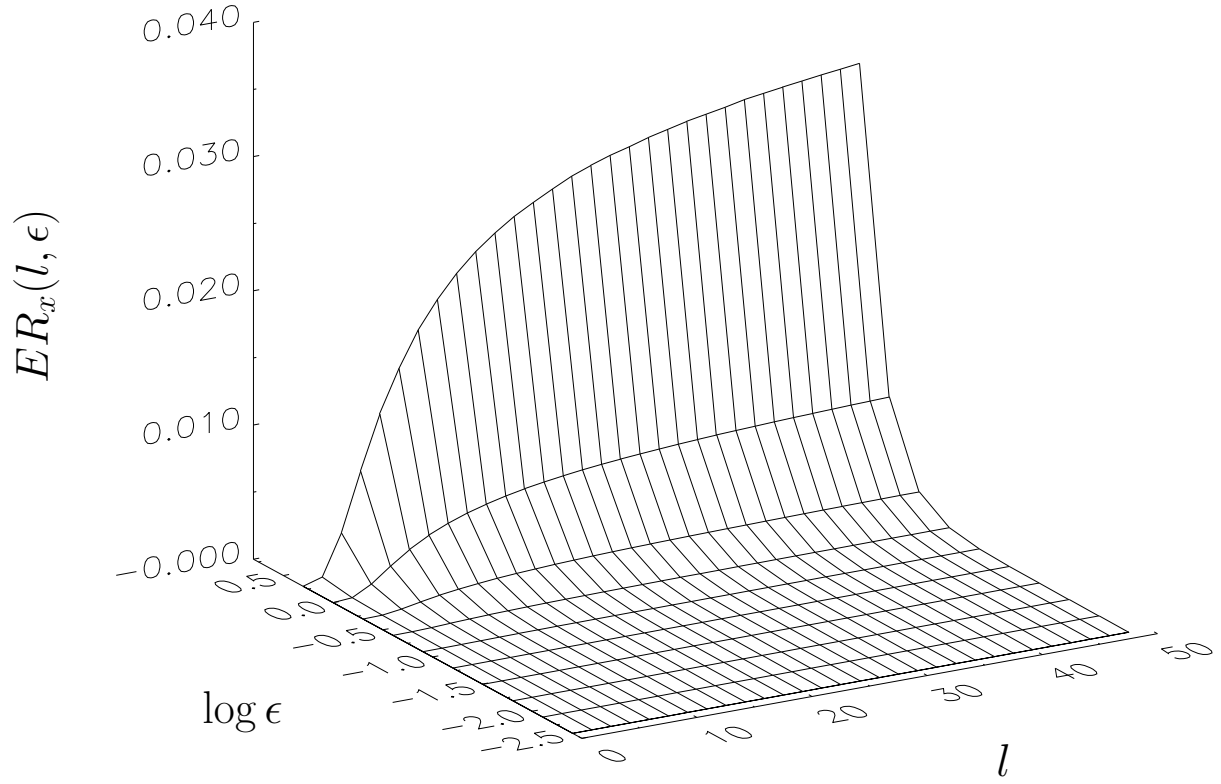

Figure 9 The relative errors $EL(l,\epsilon)$ and $ER_x(l,\epsilon)$. Note that the errors die quickly as $\epsilon \to 0$ yet they are unbounded for large l. The errors ER_z are identical to ER_x.

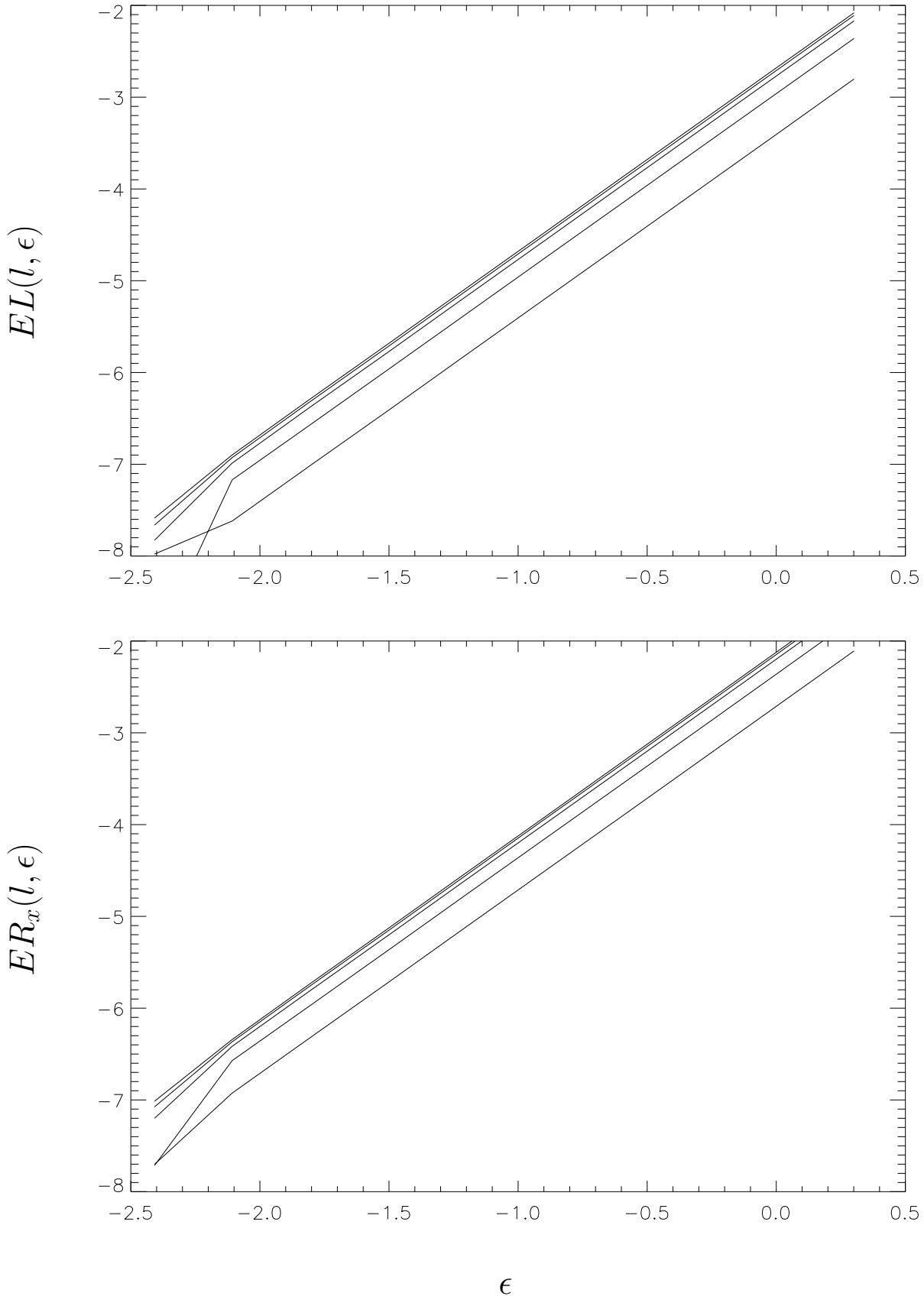

Figure 10 Cross sections of Figure (9) for various values of l. In each case the error converges quadraticly with respect to ϵ. The irregular behaviour in ER_x is probably due to round-off error. The curves correspond to $l = 5, 10, 20, 40$ and 80 with the error generally increasing with l. This applies also to Figure (12).

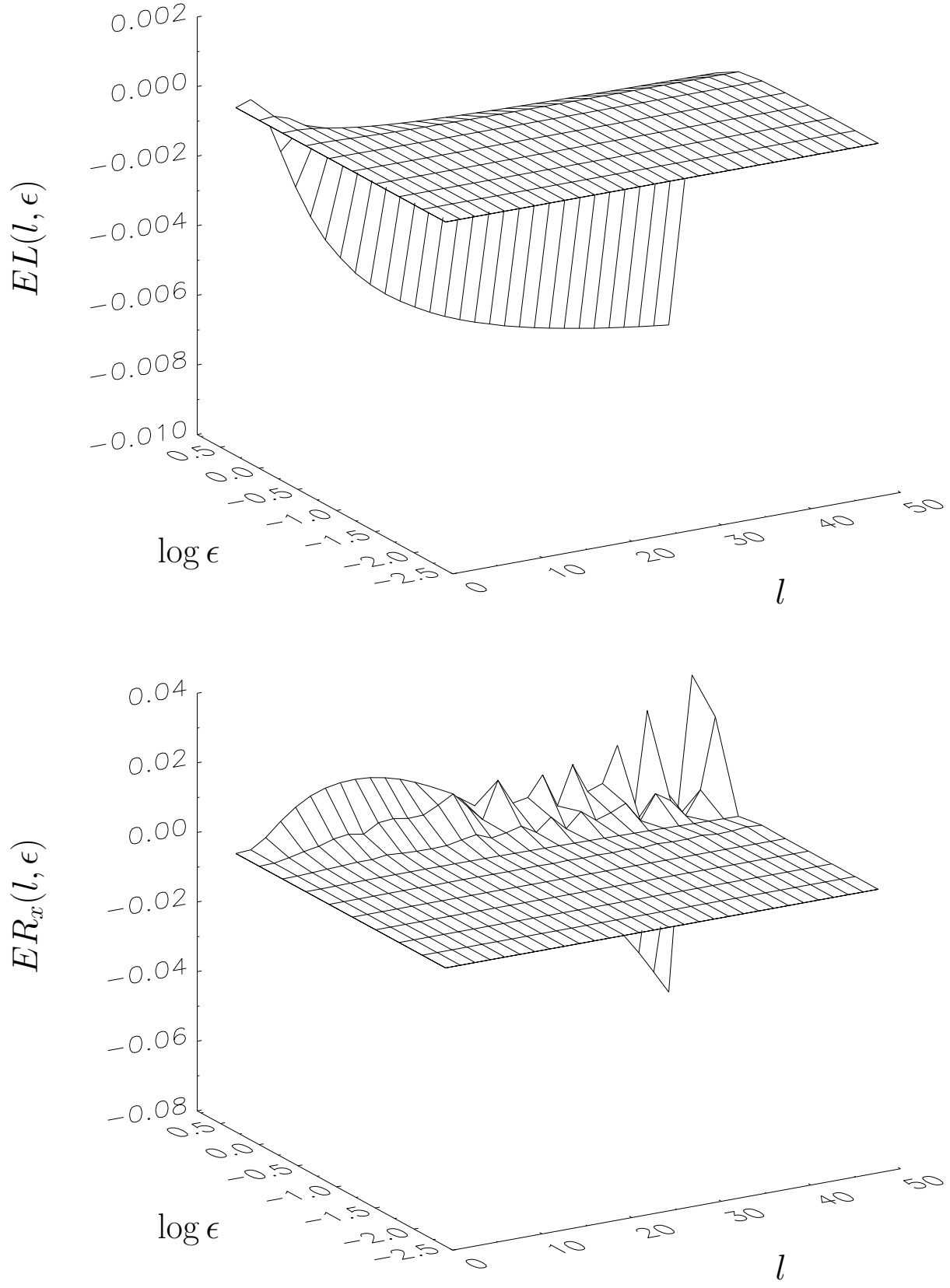

Figure 11 Errors $EL(l,\epsilon)$ and $ER_x(l,\epsilon)$ for the first variation in which the alternative inner boundary condition (3.3.1) was used. The oscillations in ER_x are not significant since $R_x \approx 10^{-5}$ at $l = 50$ and the absolute errors are very small.

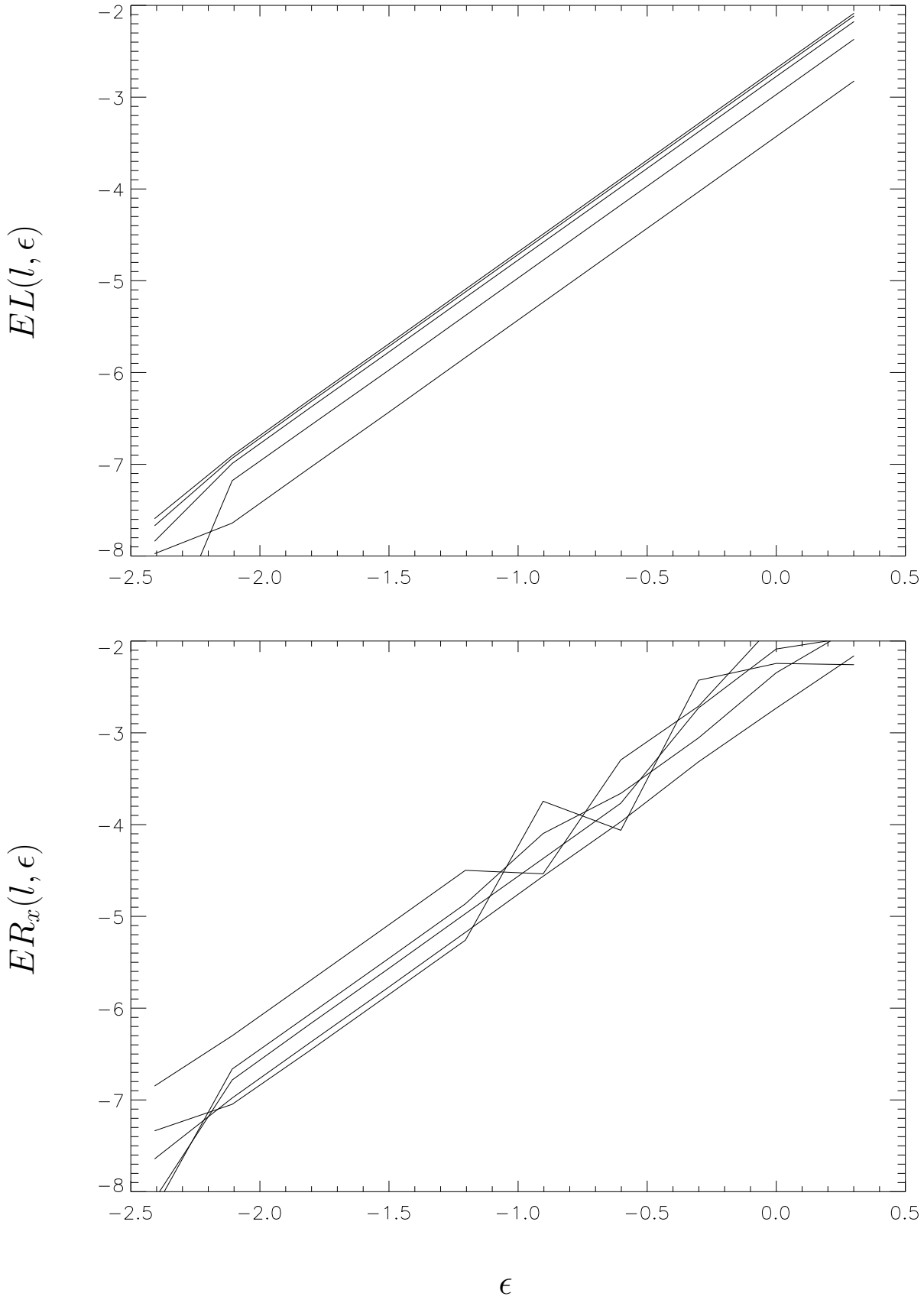

Figure 12 Cross sections of Figure (11). In each case the error converges quadraticly with respect to ϵ. The irregular behaviour in ER_x is due to the oscillations in the curvatures.

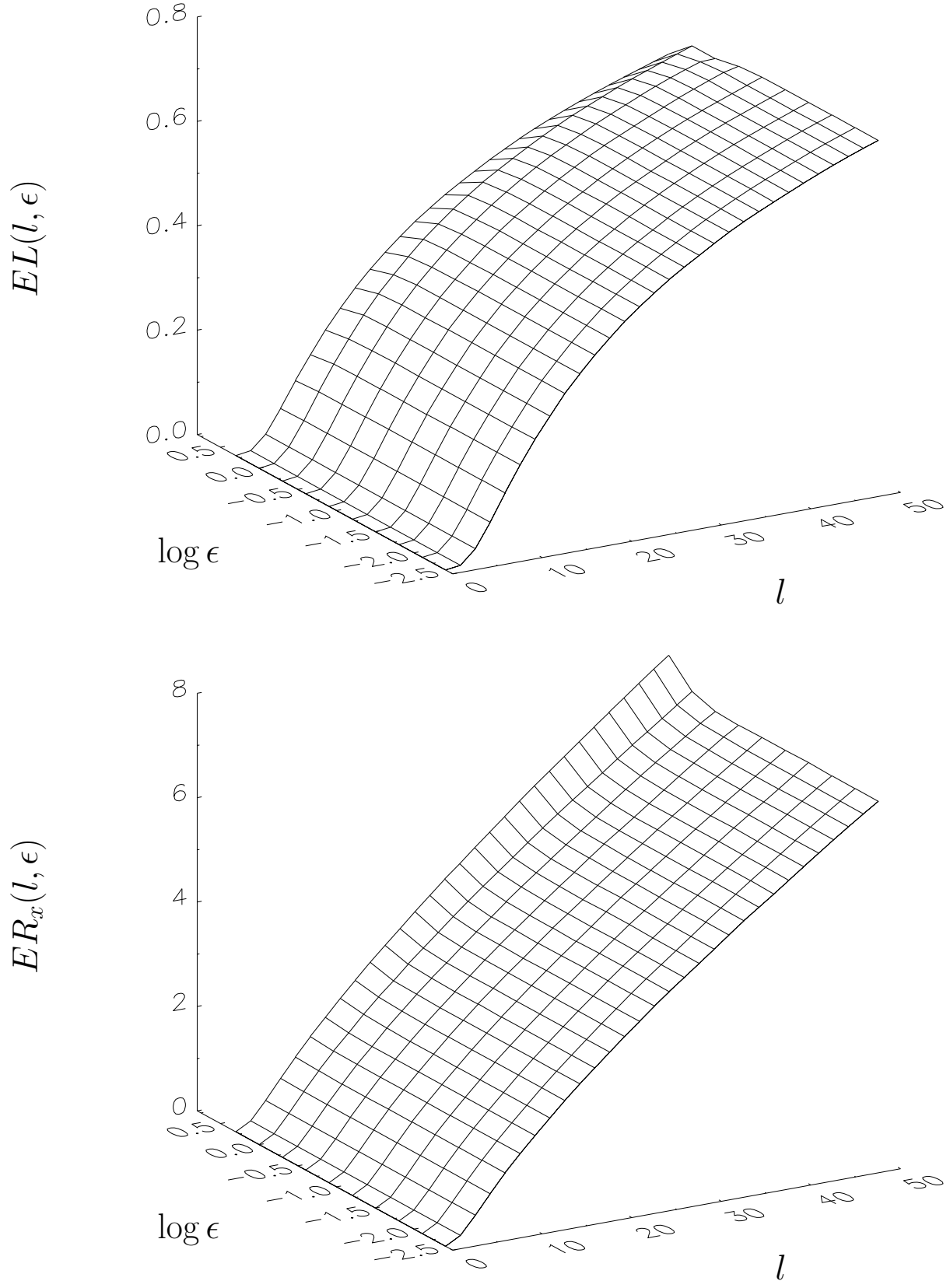

Figure 13 Errors $EL(l,\epsilon)$ and $ER_x(l,\epsilon)$ for the third variation in which successive tiles were scaled versions of previous tiles. There is no convergence in either ϵ or l.